

# Shattered Compositionality: Counterintuitive Learning Dynamics of Transformers for Arithmetic

Xingyu Zhao<sup>1</sup> Darsh Sharma<sup>1</sup> Rheeya Uppaal<sup>1</sup> Yiqiao Zhong<sup>1</sup>

## Abstract

Large language models (LLMs) often exhibit unexpected errors or unintended behavior, even at scale. While recent work reveals the discrepancy between LLMs and humans in skill compositions, the learning dynamics of skill compositions and the underlying cause of non-human behavior remain elusive. In this study, we investigate the mechanism of learning dynamics by training transformers on synthetic arithmetic tasks. Through extensive ablations and fine-grained diagnostic metrics, we discover that transformers do not reliably build skill compositions according to human-like sequential rules. Instead, they often acquire skills in reverse order or in parallel, which leads to unexpected mixing errors especially under distribution shifts—a phenomenon we refer to as shattered compositionality. To explain these behaviors, we provide evidence that correlational matching to the training data, rather than causal or procedural composition, shapes learning dynamics. We further show that shattered compositionality persists in modern LLMs and is not mitigated by pure model scaling or scratchpad-based reasoning. Our results reveal a fundamental mismatch between a model’s learning behavior and desired skill compositions, with implications for reasoning reliability, out-of-distribution robustness, and alignment. Our code is publicly available<sup>1</sup>.

## 1. Introduction

Large language models (LLMs) achieve high accuracy on various compositional benchmarks, from code generation to multi-step mathematical reasoning (White et al., 2024). However, despite strong in-distribution performance, small shifts in problem formulation can trigger brittle behavior

<sup>1</sup>University of Wisconsin–Madison. Correspondence to: Yiqiao Zhong <yiqiao.zhong@wisc.edu>.

Preprint. February 2, 2026.

<sup>1</sup>[https://github.com/PeterXingyuZhao/Arithmetic\\_Transformer](https://github.com/PeterXingyuZhao/Arithmetic_Transformer)

through reasoning that “almost” composes, but fails in unexpected ways (Song et al., 2025b). Such brittleness is especially concerning in settings that require robust reuse and recombination of learned capabilities, with direct implications for alignment and safety (MacDiarmid et al., 2025).

A natural hypothesis is that such failures arise because models build and apply skill compositions differently from humans. Recent mechanistic analyses support this view: rather than implementing a single coherent procedure, LLMs often rely on multiple interacting mechanisms (sometimes complementary, sometimes competing) consistent with a “bag of heuristics” rather than a unified algorithm (Wiegreffe et al., 2024; Lindsey et al., 2025; Nikankin et al., 2025). More broadly, models can appear competent while relying on non-human internal strategies that fail under distribution shift or adversarial variation (Berglund et al., 2024; Shojaee et al., 2025). However, most prior work studies *static* snapshots of trained models. We still lack a developmental account of *how compositional structures emerge during training, and what determines the order in which constituent subskills are learned*. Without this training-dynamics view, it is difficult to diagnose why compositions become brittle, or to design interventions that shape them.

Developing a fine-grained understanding of LLM learning dynamics on narrowly defined tasks is necessary to disentangle learning mechanisms, but is currently impeded by the scale of contemporary models and data. We aim to address this gap by training small transformers on synthetic arithmetic tasks. Arithmetic is a clean compositional domain with well-specified rules and minimal semantic ambiguity, and it has long served as a testbed for understanding learning dynamics (e.g., grokking and length generalization) (Dziri et al., 2023; Power et al., 2022; Anil et al., 2022; Kazemnejad et al., 2023) and for prototyping training paradigms (Lee et al., 2025; Panigrahi et al., 2025). Crucially, arithmetic admits fine-grained, mechanistically meaningful diagnostics. We decompose tasks into subskills (e.g., digit-wise prediction, carry handling) and track their acquisition across training, enabling a direct view of how compositions form and how they fail.

LLMs are believed to represent compositions through “skill graphs” (Arora & Goyal, 2023; Lindsey et al., 2025), but

the learning dynamics of such skill compositions remain opaque. Our central empirical finding is that transformers do not reliably acquire subskills according to human-like sequential rules; instead, they frequently learn in *reverse order* (e.g., higher-place digits before lower-place digits) or acquire multiple subskills *in parallel*. Parallel acquisition can induce *competition* between subskills, which in turn yields characteristic *mixing errors*—failures where parts of different learned behaviors are recombined inconsistently—especially under distribution shifts. We refer to this training-dynamics failure mode as **shattered compositionality**. Importantly, shattered compositionality is not merely a curiosity of synthetic training: LLM deployments routinely involve distribution shifts induced by prompt formats and small wording changes, and such shifts can degrade performance (Selar et al., 2024; Mirzadeh et al., 2025; Chatziveroglou et al., 2025) and create new safety risks (Ren et al., 2025).

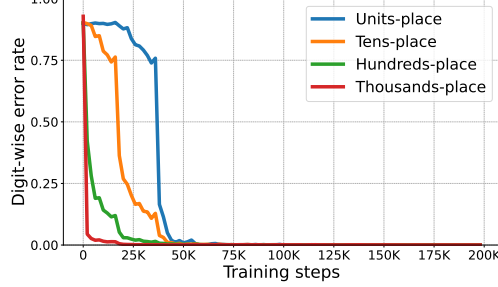
What drives these counterintuitive learning trajectories? We provide evidence for a simple explanatory hypothesis: learning dynamics are shaped primarily by *correlational matching* to the training distribution, rather than by discovering a causal or procedural decomposition of the underlying rules. This framing is consistent with the view that models may represent compositional behavior via interacting skill graphs or constituent mechanisms rather than a single algorithm. Concretely, we show that the emergence of specific subskills aligns with correlational signals (captured by information-theoretic quantities) available early in training; once those signals are saturated, additional subskills become learnable. Our analysis offers a plausible explanation for why learning can proceed in reverse, why parallel skills can interfere, and why small distribution shifts can expose brittle compositions despite high training accuracy.

Overall, our contributions can be summarized as follows:

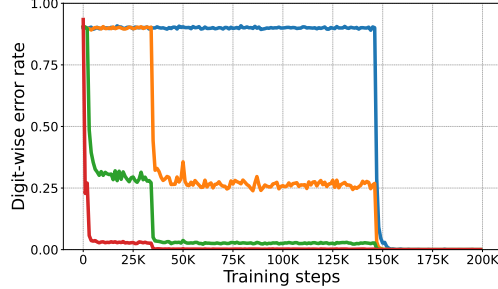
- We characterize training dynamics of compositional subskills, revealing reverse-order and parallel learning in transformers.
- We identify **shattered compositionality**: competition-induced mixing errors amplified by distribution shifts.
- We show learning dynamics align with correlational statistics of the data, explaining non-human learning order.
- We demonstrate that these failures persist in modern LLMs and resist mitigation via scaling or scratchpads.

## 2. Related Work

**Static analyses of arithmetic and reasoning.** A growing body of work in mechanistic interpretability seeks to identify task-relevant components in trained neural networks (Elhage et al., 2021; Olsson et al., 2022; Hendel et al., 2023; Song



(a) Digit-wise error in plain output format



(b) Digit-wise error in reverse output format

**Figure 1. Transformers learn digits in non-human order for addition regardless of output formats.** We train transformers on addition of the format  $a + b + c + d = e$  with multiple-digit input integers  $a, b, c, d$ , and evaluate the digit-wise error rates of  $e$  across 200K training steps. In contrast to human’s natural order, models learn from higher digits to lower digits. This non-human order remains so even when we reverse the digit order of output  $e$  which incentivizes the model to follow the human’s order.

et al., 2025a). For arithmetic, prior studies have shown that specific attention heads, MLPs, or low-dimensional activation subspaces coordinate to carry out computation (Stolfo et al., 2023; Zhang et al., 2024; Zhou et al., 2024; Hu et al., 2025). Notably, Lindsey et al. (2025) identify complementary mechanisms for addition—one encoding coarse magnitude and another handling unit-place computation. Nikankin et al. (2025) show that arithmetic is implemented via a “bag of heuristics”, where constituent skills are represented in a parallel fashion, rather than a unified algorithm. These results suggest that arithmetic behavior arises from multiple interacting mechanisms rather than a single procedural rule, consistent with non-human internal representations. However, nearly all such analyses operate on *static, trained models*. As a result, they cannot explain how these mechanisms emerge during training, how learning order is determined, or how interactions between partially learned skills lead to downstream failures.

**Learning dynamics on arithmetic without decomposition.** Synthetic arithmetic tasks have long been used to probe learning dynamics in neural networks. Power et al. (2022) identify grokking, where generalization emerges abruptly after extended overfitting, inspiring follow-up work on representation dynamics and weight evolution (Nanda

Table 1. Summary of synthetic tasks.

	ADDITION	MULTI	COMPARISON	SORTING
VOCAB SIZE	15	15	18	15
MAX SEQ LEN	21	85	12	40
SAMPLE SIZE	1M	100K	45K	100K

et al., 2023; Liu et al., 2022; Mallinar et al., 2024). Other studies examine how input format, curriculum design, or recursive training affect arithmetic generalization (Lee et al., 2024; 2025). While these works characterize *when* models generalize or *whether* specific training strategies help, they typically treat arithmetic as a monolithic task. They do not decompose problems into constituent subskills or track how those subskills are acquired over time. Consequently, existing training-dynamics analyses cannot explain learning order, parallel skill acquisition, or interference effects—phenomena central to shattered compositionality.

**Skill composition and its limits in language models.** Recent theoretical and empirical work suggests that LLMs solve complex tasks by composing simpler skills. Arora & Goyal (2023) propose that models form skill graphs whose nodes correspond to reusable subroutines, while Lindsey et al. (2025) present attribution-graph analyses showing that learned compositions can involve cooperative or competing mechanisms. At the same time, several studies argue that statistical matching fundamentally limits the compositional generalization of LLMs (Dziri et al., 2023; Abbe et al., 2024; Abedsoltan et al., 2025; Wang et al., 2025). However, this line of work primarily characterizes *what* skill compositions look like after training, or *why* certain compositions may fail in principle. It does not explain how non-human compositions arise from gradient-based training, nor how competition between partially learned skills leads to brittle behavior under distribution shift. Our work addresses these questions by directly analyzing the emergence and interaction of subskills during training.

In summary, prior work studies mechanisms, learning dynamics, and skill composition largely in isolation, whereas we connect all three by analyzing how compositional subskills *emerge and compete* during training.

### 3. Experimental Setup

We consider 4 synthetic experiments where we train small transformers for arithmetic tasks. Following Power et al. (2022); Lee et al. (2024), we use digit-wise tokenization where integers are converted to multiple digit-tokens in  $\{0, 1, \dots, 9\}$ , and operators and delimiters such as ‘+’, ‘=’, ‘×’, ‘>’, ‘<’, ‘,’ are treated as separate symbol-tokens.

#### 3.1. Tasks and data generation

**Addition task.** For the 4-operand addition task, we sample training examples of the following format  $a + b + c + d = e$ ;

for instance,

$$\underbrace{349}_{a} + \underbrace{102}_{b} + \underbrace{382}_{c} + \underbrace{907}_{d} = \underbrace{1740}_{e} \quad (\text{plain format})$$

where  $a, b, c, d$  are uniformly drawn from  $\{0, 1, \dots, 999\}$ , and  $e$  is the correct result. Following the setting of Lee et al. (2024), we tokenize every character of the input sequence. For example, “349” is encoded by three separate tokens, and “+”, “=” are encoded by two other tokens. We view subskills as predicting individual digits in the output.

Following Lee et al. (2024), we also consider the *reverse output format* where the order of digits in the output is reversed. This reverse format is consistent with the human’s arithmetic rule since carry is determined by lower digits and used in higher digits.

$$\underbrace{349}_{a} + \underbrace{102}_{b} + \underbrace{382}_{c} + \underbrace{907}_{d} = \underbrace{0471}_{e'} \quad (\text{reverse format})$$

For evaluation, our test data has the same format as training data. We still interpret the digits using the original order; for example, we treat “1” in  $e'$  as the thousands-place digit.

**Simple multiplication task.** The format of training examples is  $a \times b = c$ , where  $a$  is a multiple-digit integer,  $b$  is a single-digit integer, and  $c$  is the correct result. For example,

$$\underbrace{345901}_{a} \times \underbrace{8}_{b} = \underbrace{2767208}_{c}.$$

We first sample the length  $\ell$  for  $a$  from  $\{1, \dots, 40\}$  and then use uniform sampling to generate  $a$  and  $b$ : we sample  $a$  uniformly from  $\{0, 1, \dots, 10^\ell - 1\}$  and  $b$  uniformly from  $\{0, 1, \dots, 9\}$ . We also consider the reverse output format where the output digits are arranged in the reverse order; for example,  $c$  above is represented by “8027672” instead.

**Comparison task.** In the comparison task, the model predicts the relationship token  $r \in \{>, <, =\}$  between two comma-separated 4-digit integers  $a$  and  $b$ . An example input sequence is formatted as:

$$\underbrace{5293}_{a}, \underbrace{5241}_{b} \rightarrow \underbrace{>}_{r}$$

where we tokenize every character as before. We consider two sampling strategies for generating the training data: (i)

**Uniform sampling.** We uniformly sample  $a$  and  $b$  from  $\{1000, 1001, \dots, 9999\}$ . We note that the probability of two numbers sharing leading digits decays rapidly (e.g., only 1% of pairs share both thousands and hundreds digits), thus inadequately representing “hard” examples. (ii)

**Balanced sampling.** To address the scarcity of “hard” examples in uniform sampling, we generate a dataset of 5 equiprobable groups defined by the *Number of Controlled Identical Digits* (NCID). The  $\text{NCID} \in \{0, 1, 2, 3, 4\}$  is the

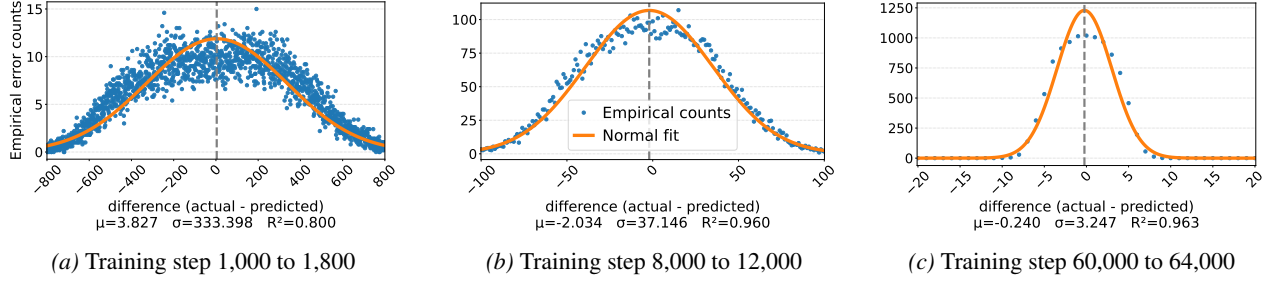


**Figure 2. Transformers learn addition similar to an improving approximation algorithm**, narrowing the error spread as training continues. When training the model for addition in reverse format, we compare the model’s predicted integer  $\hat{e}$  and the groundtruth integer  $e'$ . The scatterplots are instances of the difference  $e' - \hat{e}$  collected over three intervals. We then fit a normal distribution for each scatterplot. Despite trained on raw digits, the model learns to approximate the correct solution with increasingly smaller Gaussian error.

leftmost position where the digits in  $a, b$  are guaranteed to be identical (0 means no digits are controlled). To be more specific, letting  $a = a_1a_2a_3a_4$  and  $b = b_1b_2b_3b_4$  be the digit-wise representation of  $a$  and  $b$ , we generate the group ( $0 \leq k \leq 4$ ) with NCID =  $k$  by conditioning on  $a_j = b_j$  for  $j \leq k$  and uniformly sampling remaining digits in  $a$  and  $b$ . Note that the last group consists of identical pairs ( $a = b$ ) and thus 20% of training examples contain token “=”. See Section A.2 for a detailed description.

**Sorting task.** The training examples take the following format  $a, b, c, d \rightarrow \text{sorted}(a, b, c, d)$ , where  $a, b, c, d$  are either 3-digit or 4-digit integers. For instance,

$$\underbrace{9312}_{a}, \underbrace{4661}_{b}, \underbrace{405}_{c}, \underbrace{6252}_{d} \rightarrow \underbrace{405}_{c}, \underbrace{4661}_{b}, \underbrace{6252}_{d}, \underbrace{9312}_{a}.$$

For data generation, we mainly focus on a *doubly balanced* sampling strategy. This sampling is balanced in two aspects. (i) Length-balanced: each integer has 1/2 probability to be 3-digit, and 1/2 probability to be 4-digit; (ii) Closeness-balanced: similar to the comparison task, the generated dataset consists of 3 equiprobable groups with  $\text{NCID} \in \{0, 1, 2\}$ . See Section A.3 for details about data generation and Section C.4.1 for an alternative sampling strategy.

### 3.2. Model and Training

We use the NanoGPT architecture (Karpathy, 2022a) with standard model configurations. Unless specified otherwise, the models have 6 layers, 6 attention heads, embedding dimension 384, totaling 10.63M parameters. We use absolute positional encoding by default. We adopt the standard autoregressive training using the AdamW optimizer (Loshchilov & Hutter, 2019), with learning rate 0.001, batch size 512, and dropout 0.2. For simplicity, each input sequence contains exactly one training example, which is right-padded to a fixed maximum sequence length. For generation, we use sampling with temperature 0.8.

**Alternative setups.** To test the robustness of our results, we consider variants of our model/training setup. (i) Format of input sequences: randomly chunked input sequences.

We concatenated all training examples and then randomly selected a fixed-length window as an input sequence. (ii) Positional encoding: rotary positional embedding (RoPE) (Su et al., 2024) and T5-style relative positional embedding (Raffel et al., 2020). (iii) Decoding scheme: greedy decoding (namely top- $k$  decoding with  $k = 1$ ). We find that the results remain largely similar to our default setup; see Section C.1.1–C.1.5.

## 4. Counterintuitive Learning Dynamics of Arithmetic Subskills

### 4.1. Addition

**Digits are learned in a non-human sequential order.** Solving addition requires correct implementation of modular addition together with carry operations. Because carry represents the contribution of a lower digit place to a higher one, a natural human learning strategy is to master the unit place first and proceed sequentially toward higher digit places. Prediction at higher digit places is inherently more complex as it depends on more input digits.

In contrast to this human learning rule, the models acquire digit-level subskills in the opposite order: training consistently begins with the most significant digit and then progresses toward lower digits (Figure 1). This learning behavior is not dependent on output formats: even when we use the reverse output format (Figure 1b) which explicitly incentivizes learning from the unit place digit due to autoregressive training, the model still follows its preferred learning order. Indeed, the sharp error drops at four distinct training thresholds, together with slower overall convergence, indicate persistent conflict between the model’s intrinsic learning order and the imposed output format.

**Model behaves as a numerical approximation algorithm despite trained on raw digits.** During training, we calculate the difference  $e' - \hat{e}$  between the groundtruth integer  $e'$  and the model’s predicted integer  $\hat{e}$ . In Figure 2, we report the distribution of error counts aggregated over evaluation checkpoints within three distinct training windows.

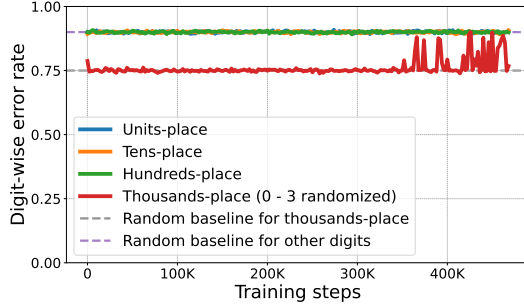


**Figure 3. Ablation experiments show randomizing higher digits disables learning.** We train transformers with modified training data for addition with the reverse format, where the thousands-place digits are replaced by uniform digits in  $\{0, 1, 2, 3\}$ . The model fails to learn any lower digit, whose digit-wise error rates are not better than random baseline.

By analyzing errors at the integer level, we examine whether the model develops a notion of integers despite trained on character-level digits.

We find that the model’s predictions approximate the groundtruth integers, with errors close to normally distributed. As training progresses beyond the critical thresholds of sharp decline in digit-wise errors (Figure 1b), the variance of the prediction errors decreases and the distribution correspondingly narrows. This indicates that the model encodes integers in an approximate, progressively refined manner, despite the discrete algebraic relationship (cyclic group) between the digits.

**Ablation experiments show that most significant digits critically initiates learning.** We consider a minor modification to the training data (under reverse format) by ablating the most significant digit. Specifically, we replace the groundtruth thousands-place digit in  $e'$  with a new uniformly sampled digit from  $\{0, 1, 2, 3\}$ , and train a transformer under the same setup. We also conduct a parallel experiment in which the hundreds-place digit is ablated. These experiments test whether disrupting learning at higher digit places impedes the acquisition of lower-digit subskills.

We find that learning lower digits depends critically on first learning higher digits. As shown in Figure 3 and 14a, the model struggles to learn the lower digits. Even after 400K training steps, the digit-wise test error rates still hovers around 90% (random baseline) for most digits. A similar phenomenon is observed under the plain output format, where learning lower digits either fails entirely or is substantially delayed; see Section C.1.5.

## 4.2. Simple Multiplication

### Model learns digits in both directions simultaneously.

To study learning order for longer integers, we sample  $a$  with maximum length 40 in the multiplication task  $a \times b =$

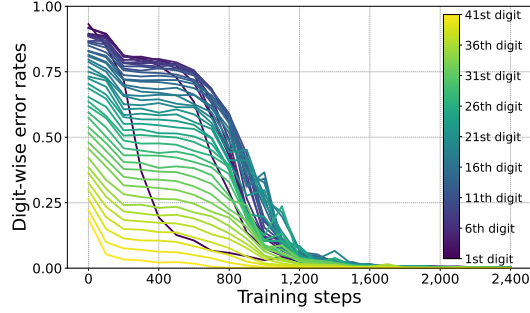


**Figure 4. Transformers learn digits in two-way order for simple multiplication.** From the evolution of digit-wise error rates, we find two opposite sequential orders are learned simultaneously. (i) Reverse order: starting from the 41st (highest) digit to the 3rd digit; (ii) Normal order: starting from the 1st (lowest) digit.

$c$ , so that the output integer  $c$  (under reverse format) can have up to 41 digits. Solving this task requires modular multiplication and carry. Compared with 4-operand addition, this task involves fewer operands but longer integers, and the carry values span a larger range  $\{0, 1, \dots, 8\}$ .

The digit-wise error rates in Figure 4 show that learning dynamics follow neither the human rule (from lowest to highest digit) nor a reverse sequential order (from highest to lowest). Instead, the model learns digits in a bidirectional manner. While learning progresses from the most significant digit toward lower digits, the unit-place digit is acquired rapidly in parallel, reaching near-zero error earlier than many higher digits. This behavior is consistent across different integer lengths  $\ell$  and output formats (Section C.2). Our results show that the model’s learning dynamics can be non-monotonic and difficult to anticipate: unlike the unidirectional order for addition, multiplication exhibits simultaneous learning in bidirectional order.

## 4.3. Comparison

### Learning multiple skills in parallel creates competitions.

A natural question from the previous task is: does learning multiple skills in parallel create synergistic or antagonistic effects? For the comparison task, we will evaluate learning dynamics using additional test examples which we call *contrast pairs*. Unlike the training distribution, we construct contrast pairs  $(a, b)$  such that the digits differ *only* at digit index  $k$  for each  $k \in \{1, \dots, 4\}$ , which is a form of distribution shifts. One example with  $k = 3$  is  $3590, 3520 \rightarrow >$ ; see Appendix C.3.1 for detailed descriptions. The resulting 4 test groups allow us to separate a model’s learning dynamics for individual digits.

The digit-wise error rates show that the model acquires subskills in parallel and thus exhibits no sequential order (Figure 20). Interestingly, evaluating the model on 4 test groups of contrast pairs (Figure 5) reveals a non-monotone learning trend at the thousands-place digit: (i) initially (be-

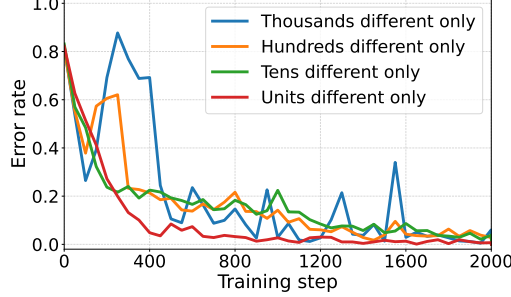


**Figure 5. Contrast pairs reveal competition between learning multiple skills for the comparison task.** We use 4 test groups of contrast pairs (differing in single digits) to evaluate the model’s ability to distinguish similar integers. The increase of errors at around 200 steps, particularly at thousands-place digits, suggests that learning “=” temporarily interfered learning the comparison of thousands-place digits.

**Table 2. Two dominant mixing error types in sorting.** Among the four input integers, two numbers, say 4-digit  $a = a_1a_2a_3a_4$  and  $b = b_1b_2b_3b_4$ , form recombined new integers in the output.

	ERROR CASE 1	ERROR CASE 2
SWAPPING	$a_1a_2a_3b_4, b_1b_2b_3a_4$	$a_1a_2b_3b_4, b_1b_2a_3a_4$
REPEATING	$a_1a_2a_3b_4, b_1b_2b_3b_4$	$a_1a_2b_3b_4, b_1b_2b_3b_4$

fore 200 steps) the model prioritizes learning comparison of the highest digits, which yields a low error; (ii) from 200–500 steps, the model learns to predict “=” based on identical digits, which counteracts the comparison skill and yields a high error; (iii) after 500 steps, the model learns all skills correctly eventually. This figure suggests the brief tension when multiple skills are learned in parallel.

#### 4.4. Sorting

**Learning parallel skills can lead to unexpected mixing errors.** Building on our analysis of skill competition, we examine parallel learning dynamics among multiple subskills, including identifying integer length and sorting individual digits. As with comparison, Figure 6 shows that subskills are learned simultaneously. We find the model exhibits persistent *mixing errors* throughout training: it fails to preserve input integers as coherent wholes, instead producing new output integers by mixing fragments of input integers. Table 2 shows two dominant types of mixing errors. This phenomenon indicates the fragility of the model’s learned compositions: the parallelism of the model’s learning dynamics can cause unintended behavior in the output.

**Skill competition can exacerbate performance degradation.** Similar to the comparison task, we design test examples to isolate the competition effects of two subskills. Denote by  $\text{sgn}(z)$  the sign function that returns 1 if  $z > 0$ , 0 if  $z = 0$ , and  $-1$  if  $z < 0$ . For two digit pairs  $(b_i, c_i), (b_j, c_j)$ , we say that they are *conflicting*

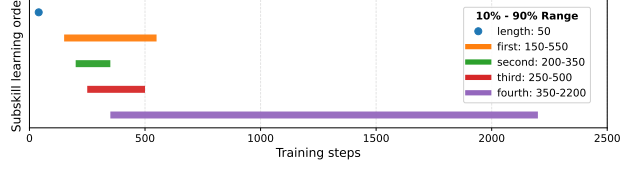


**Figure 6. Progress bars show concurrent learning of multiple skills for sorting.** We decompose sorting into five skills: crude lengths of integers, and four digit-wise ranks. The model learns the crude length (where to output the delimiter, e.g., comma) early in training, and then learn the four digit-wise skills concurrently.

if  $\text{sgn}(b_i - c_i) \cdot \text{sgn}(b_j - c_j) = -1$  and *agreeing* if  $\text{sgn}(b_i - c_i) \cdot \text{sgn}(b_j - c_j) = 1$ . We craft test examples by fixing  $a = 1000, d = 9999$  and sampling 4-digit  $b, c$  randomly conditioning on  $b_1 = c_1, b_3 = c_3$ , and  $(b_2, c_2)$  and  $(b_3, c_3)$  are either conflicting or agreeing. We assess the interaction of two skills that encode either the opposite (conflicting pair) or the same (agreeing pair) comparison relationship. Table 3 shows worse performance in the conflicting group than in the agreeing group at the end of training (9500–9950 steps), indicating that competition between oppositely directed subskills amplifies mixing errors and degrades performance.

## 5. Understanding Shattered Compositionality

To understand the learning behavior, We devise information-theoretic metrics to capture the correlational structures of the training data. We hypothesize that such statistics serve as learnable “signals” that guide the model to build compositions. We focus on the addition task under reverse format.

**Mutual information metrics.** Since all tokens live in the discrete space, a natural way to quantify the input-output correlational structure is the mutual information. Because  $a, b, c, d$  play exchangeable roles, we will focus on the relationship between input integer  $a = a_1a_2a_3$  and output integer  $e = e_0e_1e_2e_3$  where smaller subscripts mean higher digit places. Note that  $e_0$  takes values in  $\{0, 1, 2, 3\}$  and all other digits take values in  $\{0, 1, \dots, 9\}$ . Below we treat all digits as random variables drawn from uniform sampling.

Inspired by Dziri et al. (2023), we use mutual information (MI)  $I(a_i, e_j)$  to measure the correlation at the digit level. A zero MI means that the digit pair is statistical independent, whereas a nonzero  $I(a_i, e_j)$  provides learnable signals. Unfortunately, as shown in Theorem 5.1,  $I(a_i, e_j) = 0$  for all  $j > 0$  except the highest digits  $i = 1, j = 0$ . To devise non-trivial metrics, we consider the conditional MI  $I(a_i, e_i | c_{i-1})$  for  $i = 1, 2, 3$  where  $c_{i-1} \in \{0, 1, 2, 3\}$  denotes the carry to the digit  $e_{i-1}$ . Intuitively, this conditional MI quantifies the correlation between input-output digit pairs conditioning on the carry to the higher digit—which is a skill a model has likely already acquired when it learns in reverse order.

**Table 3. Evaluating the interaction of two skills for the sorting task.** Both groups (as test data under distribution shifts) yield higher error rates compared with the final test error (1.7%). Furthermore, the model produces mixing errors (swapping or repeating) significantly more often on conflicting group than on agreeing group, showing two skills with opposite effects worsen performance.

GROUP	EXAMPLE INPUT	CONDITION	MIXING ERROR	ERROR SD
CONFLICTING	1000, 6589, 6682, 9999	CONFLICTING IN $(b_2, c_2)$ AND $(b_4, c_4)$	6.63%	0.46%
AGREEING	1000, 6582, 6689, 9999	AGREEING IN $(b_2, c_2)$ AND $(b_4, c_4)$	3.61%	0.58%

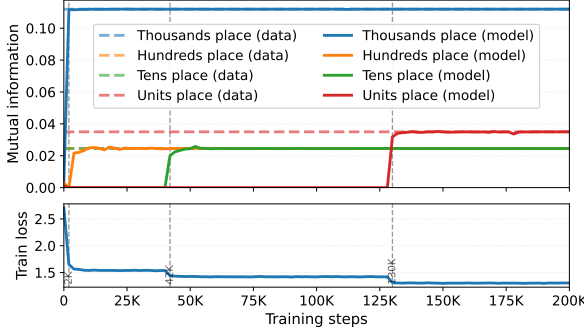


**Figure 7. Transformer’s learning behavior is captured by mutual information (MI) metrics.** **Top:** We track the MI metrics  $I(a_1, \hat{p}_0)$  (highest digit) and  $I(a_i, \hat{p}_i|c_{i-1})$  (other digits) using the model’s prediction probabilities across training (solid curves), which are compared against the corresponding  $I(a_1, e_0)$  and  $I(a_i, e_i|c_{i-1})$  based on the training data (dashed line). **Bottom:** Sharp descents of training loss are matched with changes of MI metrics at each output digit, indicating skill acquisition.

The following theorem states that learnable correlational signals are captured by appropriate information metrics capture. See Appendix F for the proof.

**Theorem 5.1.** *Under uniform sampling, we have  $I(a_1, e_0) > 0$  and  $I(a_i, e_j) = 0$  for  $j > 0$ . Moreover,  $I(a_i, e_i|c_{i-1}) > 0$  for  $i = 1, 2, 3$ .*

**Learning dynamics is consistent with correlational matching.** Given a test example, we extract the probabilities  $\hat{p}_0, \hat{p}_1, \hat{p}_2, \hat{p}_3 \in \mathbb{R}^{10}$  of predicting the 4 output digits  $e_1, e_2, e_3, e_4$ . To examine whether the model learns the correlational structure of the training data, we estimate  $I(a_1, \hat{p}_0)$  and  $I(a_i, \hat{p}_i|c_{i-1})$  for  $i = 1, 2, 3$  using test examples and track their evolution across the training process. Then, we compare these metrics against  $I(a_1, e_0)$  and  $I(a_i, e_i|c_{i-1})$  estimated from the training data.

Figure 7 shows that the sharp loss descents occur exactly at training steps where the model learns to match training-data-based MI metrics. This suggests that the model internalizes the correlational structures of training data by mirroring the MI metrics through its prediction probabilities. Based on this result, we may explain the non-human learning order as follows: the model finds nonzero signal  $I(a_1, e_0)$  early during training as other  $I(a_i, e_j)$  provide no learnable signals. Then, the model builds  $I(a_i, \hat{p}_i|c_{i-1})$  in the reverse order from  $i = 1$  to  $i = 3$ , since  $a_i$  and  $e_i$  are conditionally cor-

related given its acquired skill (carry  $c_{i-1}$ ) at a higher digit place. Figure 16 shows that sharp descents of digit-wise errors also correspond exactly to the critical steps where sharp ascents of MI occur.

## 6. Brittle Compositionality Under Distribution Shift

Do LLMs struggle with similar shattered composition? To investigate robustness under distribution shift, we curate 50 templates from GSM8K benchmark by randomly selecting 50 questions involving multi-operand addition and extending each question with additional clauses. For example, a question starts with “Billy sells DVDs. He has 8 customers on Tuesday. His first 3 customers buy one DVD each” and asks for total DVDs sold. We add 1–6 clauses with the structure “his next  $m$  customers buy  $k$  DVDs each” where  $m, k$  are random positive integers. The added clauses increase the number of operands in the final summation. Refer to Section D for template details.

We evaluate 10 open-source LLMs using our templates. Figure 8 shows that all models, including instruction-finetuned or math-finetuned models, worsen as we increase the number of added clauses. One common error type is a missing or repeated term in multi-operand addition (Section D.2)—which is similar to the mixing errors in our sorting task.

Our results show that, despite remarkable accuracy on standard GSM8K, LLMs are likely to deteriorate in arithmetic performance under mild distribution shift. This result suggests that failure of learning correct arithmetic rules remains an obstacle to reliable generalization.

## 7. Can Scaling fix Shattered Compositionality?

Tigges et al. (2024) shows that key circuits driving internal mechanisms are consistent across scale. Further validating this, we investigate the generalizability of our results for the addition task under two forms of scaling. (i) **Model scaling:** We scale NanoGPT from 10M to 20M and 100M parameters, and additionally fine-tune the pre-trained Pythia-1B model. (ii) **Reasoning scaling:** we add a scratchpad (Nye et al., 2022) in the training examples to help models learn intermediate steps. To be specific, the training examples contain explicit decomposition of operands according to

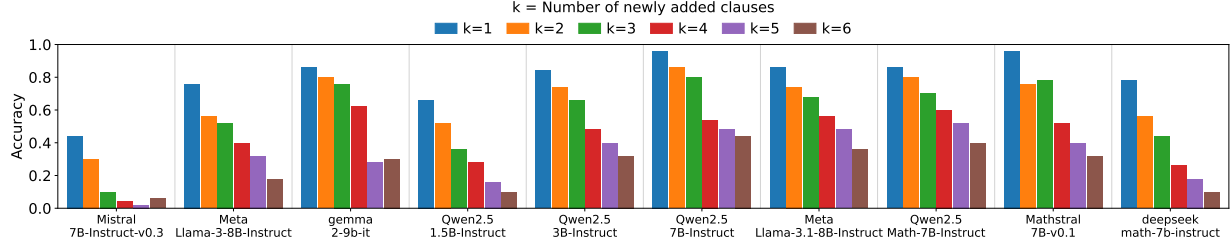


Figure 8. LLMs are susceptible to distribution shifts (extra clauses) of GSM8K data. We evaluate 10 LLMs on 50 curated templates built on selected questions from GSM8K datasets. Each template admits  $k$  new clauses ( $k = 1, \dots, 6$ ) as addends in a reasoning step. We find that both instruct-finetuned and reasoning-finetuned models have decreasing accuracy as we introduce more clauses.

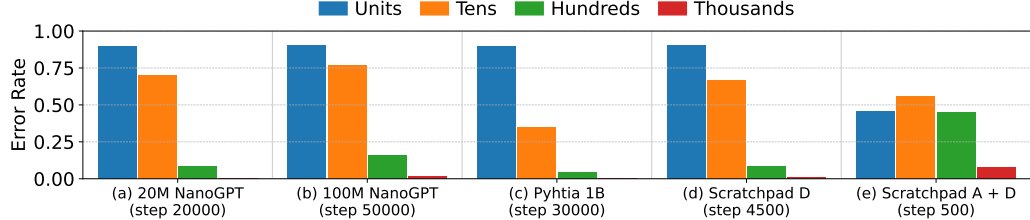


Figure 9. Effects of model scale and scratchpad on digit-wise error in addition. Each panel reports digit-wise error rates (units, tens, hundreds, thousands) at a fixed training step. Panels (a) and (b): pure model scaling when training NanoGPT from scratch. Panel (c): fine-tuning a pretrained Pythia-1B model. Panels (d) and (e): training with different scratchpad (reasoning) formats.

digit places. We conduct two experiments with different scratchpad formats (see Section E.3 for details):

$$\begin{aligned}
 811 + 856 + 239 + 313 &= 100(8 + 8 + 2 + 3) + 10(1 + 5 \\
 &+ 3 + 1) + 1(1 + 6 + 9 + 3) = 2219 \quad (\text{D scratchpad}) \\
 811 + 856 + 239 + 313 &= 100(8 + 8 + 2 + 3) + 10(1 + 5 \\
 &+ 3 + 1) + 1(1 + 6 + 9 + 3) = 100(21) + 10(10) \\
 &+ 1(19) = 2219 \quad (\text{D+A scratchpad})
 \end{aligned}$$

**Pure model scaling does not change learning behavior.** Using the existing addition data and training setup, we train two larger NanoGPT models from scratch and report a summary of results. In Figure 9, we plot digit-wise errors at 20K training steps for 20M NanoGPT and 50K steps for 100M NanoGPT. The learning progress of the 4 digit skills is consistent with our findings in Figure 1. See Section E.1 for the full dynamics of error rates.

**Beyond synthetic experiment: fine-tuning Pythia for addition.** To test whether pre-training on a large, diverse corpus impacts the learning dynamics of addition, we fine-tune the pre-trained Pythia-1B (Biderman et al., 2023) model on our 4-operand addition dataset using the same autoregressive setup as in our synthetic experiments. Treating the model as a text-to-text black box, we evaluate the decoded output digit-wise. From Figure 9 (Section E.2), Pythia-1B exhibits the same reverse learning order as in the synthetic setting. This suggests that exposure to diverse pre-training data does not enable the model to discover the human rule for addition more effectively.

**Scratchpad can be ineffective in enforcing rule learning.** Scratchpad is a form of chain-of-thought (CoT) fine-tuning that spells out reasoning traces in the training data and explicitly incentivizes models to generate reasoning steps. Complex compositional tasks are difficult for transformers to learn unless scratchpad is used (Dziri et al., 2023).

However, we find that even training with our formatted scratchpad still suffers from the persistent issue of reverse learning order, and their impact is highly sensitive to the specific format. We trained NanoGPT models from scratch using a scratchpad and evaluated digit-wise errors as before (comprehensive training configurations and detailed results are provided in Section E.3). Figure 9 (d) and (e) indicate that the non-human learning order is still exhibited, yet the exact developmental trajectory is contingent on the scratchpad configuration. These results underscore the critical role of scratchpad format in shaping a model’s learning behavior.

## 8. Limitations and Future Work

Our findings suggest that shattered compositionality is fundamentally a training-dynamics phenomenon rather than a post-hoc artifact of auditing trained models. We focus on small models and arithmetic not as an end goal, but as a microscope to reveal the intrinsic issues of autoregressive training. In future work, it would be interesting to develop practical metrics for evaluating LLMs. We are also interested in going beyond autoregressive training and studying the effects of the reinforcement learning, and propose methods to mitigate the brittleness of shattered compositions.

## Impact Statement

Our work is a foundational study of the learning dynamics of transformers. Most experiments are conducted in well-controlled synthetic settings, with limited validation on a small-scale language model (Pythia-1B). We do not introduce new model architectures or training procedures with direct misuse concerns. The primary positive impact of this work is the identification and analysis of a failure mode, namely shattered compositionality, in how transformers acquire and combine skills. Our findings offer insights relevant to the reliability and alignment of LLMs, and may lead to improvements in evaluation practices and future training methods aimed at enhancing reasoning reliability and out-of-distribution robustness. A potential negative impact is over-generalization of our conclusions, given the emphasis on synthetic tasks and small-scale model experiments. Accordingly, our results should be validated across broader task domains and model families before being used to inform policy or deployment decisions.

## Acknowledgments

Y.Z. is partially supported by NSF-DMS grant 2412052 and by a Coefficient Giving (formerly Open Philanthropy) grant. We also thank Zaid Harchaoui and Abhishek Panigrahi for helpful discussions.

## References

Abbe, E., Bengio, S., Lotfi, A., Sandon, C., and Saremi, O. How far can transformers reason? the globality barrier and inductive scratchpad. In *Proceedings of the 38th International Conference on Neural Information Processing Systems*, pp. 27850–27895, 2024.

Abedsoltan, A., Zhang, H., Wen, K., Lin, H., Zhang, J., and Belkin, M. Task generalization with autoregressive compositional structure: Can learning from  $d$  tasks generalize to  $d^t$  tasks? *arXiv preprint arXiv:2502.08991*, 2025.

Anil, C., Wu, Y., Andreassen, A., Lewkowycz, A., Misra, V., Ramasesh, V., Slone, A., Gur-Ari, G., Dyer, E., and Neyshabur, B. Exploring length generalization in large language models. *Advances in Neural Information Processing Systems*, 35:38546–38556, 2022.

Arora, S. and Goyal, A. A theory for emergence of complex skills in language models. *arXiv preprint arXiv:2307.15936*, 2023.

Berglund, L., Tong, M., Kaufmann, M., Balesni, M., Stickland, A. C., Korbak, T., and Evans, O. The reversal curse: LLMs trained on “a is b” fail to learn “b is a”. In *The Twelfth International Conference on Learning Representations*, 2024. URL <https://openreview.net/forum?id=GPKTIktA0k>.

Biderman, S., Schoelkopf, H., Anthony, Q., Bradley, H., O’Brien, K., Hallahan, E., Khan, M. A., Purohit, S., Prashanth, U. S., Raff, E., et al. Pythia: a suite for analyzing large language models across training and scaling. In *Proceedings of the 40th International Conference on Machine Learning*, pp. 2397–2430, 2023.

Chatziveroglou, G., Yun, R., and Kelleher, M. Exploring llm reasoning through controlled prompt variations. *arXiv preprint arXiv:2504.02111*, 2025.

Dziri, N., Lu, X., Sclar, M., Li, X. L., Jiang, L., Lin, B. Y., Welleck, S., West, P., Bhagavatula, C., Le Bras, R., et al. Faith and fate: Limits of transformers on compositionality. *Advances in Neural Information Processing Systems*, 36: 70293–70332, 2023.

Elhage, N., Nanda, N., Olsson, C., Henighan, T., Joseph, N., Mann, B., Askell, A., Bai, Y., Chen, A., Conerly, T., DasSarma, N., Drain, D., Ganguli, D., Hatfield-Dodds, Z., Hernandez, D., Jones, A., Kernion, J., Lovitt, L., Ndousse, K., Amodei, D., Brown, T., Clark, J., Kaplan, J., McCandlish, S., and Olah, C. A mathematical framework for transformer circuits. *Transformer Circuits Thread*, 2021. <https://transformer-circuits.pub/2021/framework/index.html>.

Hendel, R., Geva, M., and Globerson, A. In-context learning creates task vectors. In *The 2023 Conference on Empirical Methods in Natural Language Processing*, 2023.

Hu, X., Yin, K., Jordan, M. I., Steinhardt, J., and Chen, L. Understanding in-context learning of addition via activation subspaces. *arXiv preprint arXiv:2505.05145*, 2025.

Karpathy, A. NanoGPT. <https://github.com/karpathy/nanoGPT>, 2022a.

Karpathy, A. nanogpt. <https://github.com/karpathy/nanoGPT>, 2022b. [Online; accessed 14-July-2025].

Kazemnejad, A., Padhi, I., Natesan Ramamurthy, K., Das, P., and Reddy, S. The impact of positional encoding on length generalization in transformers. *Advances in Neural Information Processing Systems*, 36:24892–24928, 2023.

Lee, N., Sreenivasan, K., Lee, J. D., Lee, K., and Papailiopoulos, D. Teaching arithmetic to small transformers. In *International Conference on Learning Representations*. ICLR 2024, 2024.

Lee, N., Cai, Z., Schwarzschild, A., Lee, K., and Papailiopoulos, D. Self-improving transformers overcome easy-to-hard and length generalization challenges. In *Forty-second International Conference on Machine Learning*, 2025. URL <https://openreview.net/forum?id=ZtX0MBT6mf>.

Lindsey, J., Gurnee, W., Ameisen, E., Chen, B., Pearce, A., Turner, N. L., Citro, C., Abrahams, D., Carter, S., Hosmer, B., Marcus, J., Sklar, M., Templeton, A., Bricken, T., McDougall, C., Cunningham, H., Henighan, T., Jermyn, A., Jones, A., Persic, A., Qi, Z., Thompson, T. B., Zimmerman, S., Rivoire, K., Conerly, T., Olah, C., and Batson, J. On the biology of a large language model. *Transformer Circuits Thread*, 2025. URL <https://transformer-circuits.pub/2025/attribution-graphs/biology.html>.

Liu, Z., Kitouni, O., Nolte, N. S., Michaud, E., Tegmark, M., and Williams, M. Towards understanding grokking: An effective theory of representation learning. *Advances in Neural Information Processing Systems*, 35:34651–34663, 2022.

Loshchilov, I. and Hutter, F. Decoupled weight decay regularization. In *International Conference on Learning Representations*, 2019. URL <https://openreview.net/forum?id=Bkg6RiCqY7>.

MacDiarmid, M., Wright, B., Uesato, J., Benton, J., Kutasov, J., Price, S., Bouscal, N., Bowman, S., Bricken, T., Cloud, A., et al. Natural emergent misalignment from reward hacking in production rl. *arXiv preprint arXiv:2511.18397*, 2025.

Mallinar, N., Beaglehole, D., Zhu, L., Radhakrishnan, A., Pandit, P., and Belkin, M. Emergence in non-neural models: grokking modular arithmetic via average gradient outer product. *stat*, 1050:29, 2024.

Mirzadeh, S. I., Alizadeh, K., Shahrokhi, H., Tuzel, O., Bengio, S., and Farajtabar, M. Gsm-symbolic: Understanding the limitations of mathematical reasoning in large language models. In *The Thirteenth International Conference on Learning Representations*, 2025.

Nanda, N., Chan, L., Lieberum, T., Smith, J., and Steinhardt, J. Progress measures for grokking via mechanistic interpretability. In *The Eleventh International Conference on Learning Representations*, 2023.

Nikankin, Y., Reusch, A., Mueller, A., and Belinkov, Y. Arithmetic without algorithms: Language models solve math with a bag of heuristics. In *The Thirteenth International Conference on Learning Representations*, 2025. URL <https://openreview.net/forum?id=O9YTt26r2P>.

Nye, M., Andreassen, A. J., Gur-Ari, G., Michalewski, H., Austin, J., Bieber, D., Dohan, D., Lewkowycz, A., Bosma, M., Luan, D., Sutton, C., and Odena, A. Show your work: Scratchpads for intermediate computation with language models. In *Deep Learning for Code Workshop*, 2022. URL <https://openreview.net/forum?id=HBlx2idbkbq>.

Olsson, C., Elhage, N., Nanda, N., Joseph, N., DasSarma, N., Henighan, T., Mann, B., Askell, A., Bai, Y., Chen, A., Conerly, T., Drain, D., Ganguli, D., Hatfield-Dodds, Z., Hernandez, D., Johnston, S., Jones, A., Kernion, J., Lovitt, L., Ndousse, K., Amodei, D., Brown, T., Clark, J., Kaplan, J., McCandlish, S., and Olah, C. In-context learning and induction heads. *Transformer Circuits Thread*, 2022. <https://transformer-circuits.pub/2022/in-context-learning-and-induction-heads/index.html>.

Panigrahi, A., Liu, B., Malladi, S., Risteski, A., and Goel, S. Progressive distillation induces an implicit curriculum. In *The Thirteenth International Conference on Learning Representations*, 2025. URL <https://openreview.net/forum?id=wPMRwmytZe>.

Power, A., Burda, Y., Edwards, H., Babuschkin, I., and Misra, V. Grokking: Generalization beyond overfitting on small algorithmic datasets. *arXiv preprint arXiv:2201.02177*, 2022.

Raffel, C., Shazeer, N., Roberts, A., Lee, K., Narang, S., Matena, M., Zhou, Y., Li, W., and Liu, P. J. Exploring the limits of transfer learning with a unified text-to-text transformer. *Journal of machine learning research*, 21(140):1–67, 2020.

Ren, Q., Li, H., Liu, D., Xie, Z., Lu, X., Qiao, Y., Sha, L., Yan, J., Ma, L., and Shao, J. Llms know their vulnerabilities: Uncover safety gaps through natural distribution shifts. In *Proceedings of the 63rd Annual Meeting of the Association for Computational Linguistics (Volume 1: Long Papers)*, pp. 24763–24785, 2025.

Sclar, M., Choi, Y., Tsvetkov, Y., and Suhr, A. Quantifying language models’ sensitivity to spurious features in prompt design or: How i learned to start worrying about prompt formatting. In *The Twelfth International Conference on Learning Representations*, 2024.

Shojaee, P., Mirzadeh, I., Alizadeh, K., Horton, M., Bengio, S., and Farajtabar, M. The illusion of thinking: Understanding the strengths and limitations of reasoning models via the lens of problem complexity. *arXiv preprint arXiv:2506.06941*, 2025.

Song, J., Xu, Z., and Zhong, Y. Out-of-distribution generalization via composition: A lens through induction heads in transformers. *Proceedings of the National Academy of Sciences*, 120(20):7833–7840, 2023.

of Sciences, 122(6):e2417182122, 2025a. doi: 10.1073/pnas.2417182122. URL <https://www.pnas.org/doi/abs/10.1073/pnas.2417182122>.

Song, P., Han, P., and Goodman, N. A survey on large language model reasoning failures. In *2nd AI for Math Workshop @ ICML 2025*, 2025b. URL <https://openreview.net/forum?id=hsgMn4KBFG>.

Stolfo, A., Belinkov, Y., and Sachan, M. A mechanistic interpretation of arithmetic reasoning in language models using causal mediation analysis. In *Proceedings of the 2023 Conference on Empirical Methods in Natural Language Processing*, pp. 7035–7052, 2023.

Su, J., Ahmed, M., Lu, Y., Pan, S., Bo, W., and Liu, Y. Roformer: Enhanced transformer with rotary position embedding. *Neurocomputing*, 568:127063, 2024.

Tigges, C., Hanna, M., Yu, Q., and Biderman, S. Llm circuit analyses are consistent across training and scale. *Advances in Neural Information Processing Systems*, 37: 40699–40731, 2024.

Wang, Z., Nichani, E., Bietti, A., Damian, A., Hsu, D., Lee, J. D., and Wu, D. Learning compositional functions with transformers from easy-to-hard data. *arXiv preprint arXiv:2505.23683*, 2025.

White, C., Dooley, S., Roberts, M., Pal, A., Feuer, B., Jain, S., Shwartz-Ziv, R., Jain, N., Saifullah, K., Naidu, S., et al. Livebench: A challenging, contamination-free llm benchmark. *arXiv preprint arXiv:2406.19314*, 4, 2024.

Wiegreffe, S., Tafjord, O., Belinkov, Y., Hajishirzi, H., and Sabharwal, A. Answer, assemble, ace: Understanding how lms answer multiple choice questions. In *The Thirteenth International Conference on Learning Representations*, 2024.

Zhang, W., Wan, C., Zhang, Y., Cheung, Y.-m., Tian, X., Shen, X., and Ye, J. Interpreting and improving large language models in arithmetic calculation. In *Proceedings of the 41st International Conference on Machine Learning*, ICML’24. JMLR.org, 2024.

Zhou, T., Fu, D., Sharan, V., and Jia, R. Pre-trained large language models use fourier features to compute addition. In *The Thirty-eighth Annual Conference on Neural Information Processing Systems*, 2024. URL <https://openreview.net/forum?id=i4MutM2TZb>.

## A. Experiment Settings

### A.1. Models and training

We performed our primary experiments using a Transformer based on the NanoGPT architecture (Karpathy, 2022b). Our main model consists of 6 layers and 6 attention heads, with an embedding dimension of 384. We use cosine learning rate scheduler with a linear warmup. We used the same training hyperparameters for all NanoGPT and scaled NanoGPT experiments. Table 5 details these values.

Table 4. Architectural specifications for the scaled NanoGPT models. Training hyperparameters remained consistent across all sizes.

Parameter	10M (Baseline)	20M	100M
Layers ( $n_{layer}$ )	6	12	4
Attention Heads ( $n_{head}$ )	6	12	12
Embedding Dim ( $d_{model}$ )	384	384	768
Total Parameters	~10M	~20M	~100M

Table 5. Hyperparameters for the NanoGPT (training from scratch) and Pythia-1B (fine-tuning) experiments.

Hyperparameter	NanoGPT (Default)	Pythia-1B (Fine-tune)
Optimizer	AdamW	AdamW
LR Schedule	Cosine	Cosine
Learning Rate	$1 \times 10^{-3}$	$1 \times 10^{-4}$
Min Learning Rate	$1 \times 10^{-4}$	$1 \times 10^{-5}$
Weight Decay	0.1	0.1
Betas ( $\beta_1, \beta_2$ )	(0.9, 0.98)	(0.9, 0.98)
Warmup Iterations	100	500
LR Decay Iterations	Max Iters	Max Iters
Gradient Clipping	1.0	1.0
Batch Size	512	512
Dropout	0.2	0.1

### A.2. Data generation for comparison task

Let  $a$  and  $b$  be two 4-digit integers with decimal representations  $a = a_1a_2a_3a_4$  and  $b = b_1b_2b_3b_4$ . We partition the training data by the *Number of Controlled Identical Digits* (NCID) into 5 equiprobable groups indexed by  $k \in \{0, 1, 2, 3, 4\}$ .

For a given group  $k$ , the data generation process is defined as follows:

1. **Prefix Generation** ( $1 \leq j \leq k$ ): The first  $k$  digits are forced to be identical. We sample a sequence  $p_1 \dots p_k$  uniformly from  $\{0, \dots, 9\}^k$  and assign:
$$a_j = b_j = p_j \quad \text{for } j = 1, \dots, k$$
2. **Suffix Generation** ( $j > k$ ): The remaining  $4 - k$  digits are sampled uniformly and independently for both numbers. We sample  $a_j, b_j \sim \mathcal{U}\{0, 9\}$  for  $j = k + 1, \dots, 4$ .

This sampling strategy ensures that the dataset contains a uniform distribution of “generative constraints,” preventing the model from encountering only trivial comparisons (e.g., where the first digits differ) or only identical pairs. The resulting distribution includes exactly 20% of samples where  $a = b$  (derived from group  $k = 4$ ).

Table 6 illustrates examples of pairs  $(a, b)$  generated from each NCID group.

### A.3. Data generation for sorting task

To enhance the model’s ability to sort both numbers of different lengths and close numbers like 6983, 6981, 6988, 6987, we adopt the “doubly balanced” sampling strategy. Specifically, in each example, each number has 0.5 probability to be 3-digit,

Table 6. Examples of generated pairs  $(a, b)$  for each NCID group  $k$ . The bolded digits indicate the guaranteed controlled prefix where  $a_j = b_j$ .

NCID ( $k$ )	Constraint	Generation Logic	Example $a$	Example $b$
0	No guaranteed match	$a, b \sim \mathcal{U}\{0..9\}^4$	7 2 9 1	4 8 1 3
1	$a_1 = b_1$	$a_1 = b_1$ ; others random	<b>3</b> 5 0 2	<b>3</b> 1 9 8
2	$a_{1:2} = b_{1:2}$	$a_{1:2} = b_{1:2}$ ; others random	<b>9</b> <b>2</b> 4 7	<b>9</b> <b>2</b> 0 5
3	$a_{1:3} = b_{1:3}$	$a_{1:3} = b_{1:3}$ ; last digit random	<b>6</b> <b>1</b> 8 3	<b>6</b> <b>1</b> 8 9
4	$a = b$	$a_{1:4} = b_{1:4}$	<b>5</b> <b>4</b> 2 1	<b>5</b> <b>4</b> 2 1

0.5 probability to be 4-digit. Once we have determined the length of all input numbers in that example, we randomly draw the NCID group from  $k \in \{0, 1, 2\}$ , each with probability 1/3. The prefix generation and suffix generation are the same as the procedure described in Section A.2, except that in suffix generation if a number is 3-digit, we only need to sample the remaining  $3 - k$  digits, whereas for a 4-digit number, we need to sample the remaining  $4 - k$  digits.

We list some training examples from our training data in Table 7.

Table 7. Examples of doubly balanced dataset for sorting task.  $l(a, b, c, d)$  denotes the length of the four numbers.

Length	NCID ( $k$ )	Constraint	Example input
(4, 4, 4, 4)	0	$l(a, b, c, d) = (4, 4, 4, 4)$	3888, 2374, 8914, 1858
(3, 4, 3, 4)	1	$l(a, b, c, d) = (3, 4, 3, 4)$ ; $a_1 = b_1 = c_1 = d_1$	581, 5099, 581, 5285
(3, 3, 4, 3)	2	$l(a, b, c, d) = (3, 3, 4, 3)$ ; $a_{1:2} = b_{1:2} = c_{1:2} = d_{1:2}$	255, 250, 2563, 258

#### A.4. Output generation

**Sampling for output generation.** For all the different experiments we used 0.8 as a default temperature for sampling. Apart from sampling with temperature 0.8, we also experimented with greedy decoding to validate our findings Figure 13 reports the results for the addition task with greedy decoding, which are similar to our original results Figure 1.

## B. Additional details about evaluation metrics

### B.1. Digit-wise Error

Let a collection of  $N$  test examples be indexed by  $k = 1, \dots, N$ . For each example  $k$ , let  $a^{(k)}$  denote the gold (actual) value and  $p_t^{(k)}$  the model’s prediction at training step  $t$ .

Define the digit width  $W$  to be the maximal digit length of these actuals:

$$W = \max_k |A^{(k)}|,$$

where  $|\cdot|$  denotes string length (number of digits). In particular,  $W$  equals 4 in our addition task.

For each  $k$ , let  $\tilde{a}^{(k)}$  be the width- $W$  representation of the actual obtained by left zero-padding the actual. For prediction, we truncate  $p_t^{(k)}$  to its rightmost  $W$  characters and then left zero-pad to width  $W$  to obtain  $\tilde{p}_t^{(k)}$ :

$$\tilde{a}^{(k)} = \text{zfill}_W(a^{(k)}), \quad \tilde{p}_t^{(k)} = \text{zfill}_W(\text{rightmost}_W(p_t^{(k)})).$$

Let  $d_i(x)$  denote the  $i$ -th digit from the right (e.g., for units,  $i = 1$  for tens, etc.) in the width- $W$  string  $\tilde{x}$ . The digit-wise error rate at place  $i$  for training step  $t$  is

$$E_i(t) = \frac{1}{N} \sum_{k=1}^N \mathbf{1}(d_i(\tilde{a}^{(k)}) \neq d_i(\tilde{p}_t^{(k)})), \quad i = 0, \dots, W-1,$$

where  $\mathbf{1}[\cdot]$  is the indicator function. Thus  $E_i(t)$  measures the fraction of examples whose predicted  $i$ -th-from-right digit (after truncation and padding) differs from the gold  $i$ -th-from-right digit.

## B.2. Mutual Information

While the digit-wise error tells us where the model makes mistakes, it does not capture the statistical dependencies the model may exploit between digit-positions in training examples. To probe this, we compute dataset-based mutual information (MI) as benchmarks and track the MI from model's prediction distribution:

**Digits and carries.** Each example is a 4-operand addition

$$a_1 a_2 a_3 + b_1 b_2 b_3 + c_1 c_2 c_3 + d_1 d_2 d_3 = e_0 e_1 e_2 e_3,$$

where  $a_1, a_2, a_3$  are the (hundreds, tens, units) digits of the first addend (and similarly for  $b, c, d$ ), and  $e_0, e_1, e_2, e_3$  are the (thousands, hundreds, tens, units) digits of the sum. For each column  $i \in \{1, 2, 3\}$  we define the *local carry-out* by

$$K_{i-1} = \left\lfloor \frac{a_i + b_i + c_i + d_i}{10} \right\rfloor,$$

i.e. the carry generated by the digits in column  $i$ .

**Dataset-based MI.** Given a dataset  $\mathcal{D} = \{(x^{(n)}, y^{(n)}, z^{(n)})\}_{n=1}^N$  extracted from the generated 1M addition examples, we use the empirical estimators

$$\hat{p}(x, y) = \frac{1}{N} \sum_{n=1}^N \mathbf{1}[x^{(n)} = x, y^{(n)} = y], \quad \hat{p}(x, y, z) = \frac{1}{N} \sum_{n=1}^N \mathbf{1}[x^{(n)} = x, y^{(n)} = y, z^{(n)} = z].$$

Mutual information and conditional mutual information are then

$$\hat{I}(X; Y) = \sum_{x, y} \hat{p}(x, y) \log \frac{\hat{p}(x, y)}{\hat{p}(x)\hat{p}(y)}, \quad \hat{I}(X; Y | Z) = \sum_z \hat{p}(z) \sum_{x, y} \hat{p}(x, y | z) \log \frac{\hat{p}(x, y | z)}{\hat{p}(x | z)\hat{p}(y | z)}.$$

The reported *dataset* probes are:

- Thousands:**  $\hat{I}(a_1; e_0)$ ,
- Carries:**  $\hat{I}(a_i; e_i | K_{i-1})$  for  $i \in \{1, 2, 3\}$
- Immediate higher digit :**  $\hat{I}(a_i; e_i | e_{i-1})$  for  $i \in \{1, 2, 3\}$ .

**MI from model prediction distributions.** For each example  $n$  and each output position (digit)  $i$ , let

$$\hat{p}_i^{(n)}(y) = p_\theta(E_i = y | \text{input}^{(n)})$$

be the model's softmax distribution over the output vocabulary at that position. To estimate MI between an input digit  $X$  and the model's predicted output distribution at position  $i$ , we first aggregate predictions by the value of  $X$ :

$$\bar{p}_i(y | x) = \frac{1}{|\mathcal{D}_x|} \sum_{n: x^{(n)}=x} \hat{p}_i^{(n)}(y), \quad \hat{p}(x) = \frac{|\mathcal{D}_x|}{N}, \quad \bar{p}_i(y) = \sum_x \hat{p}(x) \bar{p}_i(y | x).$$

We use the expected KL divergence as the estimator

$$\hat{I}_\theta(X; \hat{P}_i) = \sum_x \hat{p}(x) \text{KL}(\bar{p}_i(\cdot | x) \| \bar{p}_i(\cdot)), \quad \text{KL}(p \| q) = \sum_y p(y) \log \frac{p(y)}{q(y)}.$$

For conditioning on a discrete variable  $Z$  (either  $Z = e_{i-1}$  or  $Z = K_{i-1}$ ), we aggregate by  $(x, z)$ :

$$\bar{p}_i(y | x, z) = \frac{1}{|\mathcal{D}_{x,z}|} \sum_{n: x^{(n)}=x, z^{(n)}=z} \hat{p}_i^{(n)}(y), \quad \hat{p}(x | z) = \frac{|\mathcal{D}_{x,z}|}{|\mathcal{D}_z|}, \quad \bar{p}_i(y | z) = \sum_x \hat{p}(x | z) \bar{p}_i(y | x, z),$$

and compute

$$\hat{I}_\theta(X; \hat{P}_i | Z) = \sum_z \hat{p}(z) \sum_x \hat{p}(x | z) \text{KL}(\bar{p}_i(\cdot | x, z) \| \bar{p}_i(\cdot | z)).$$

The reported *model* probes are:

- Thousands:**  $\hat{I}_\theta(a_1; \hat{P}_0)$ ,
- Carries:**  $\hat{I}_\theta(a_i; \hat{P}_i | K_{i-1})$ ,
- Immediate higher digit:**  $\hat{I}_\theta(a_i; \hat{P}_i | e_{i-1})$ .

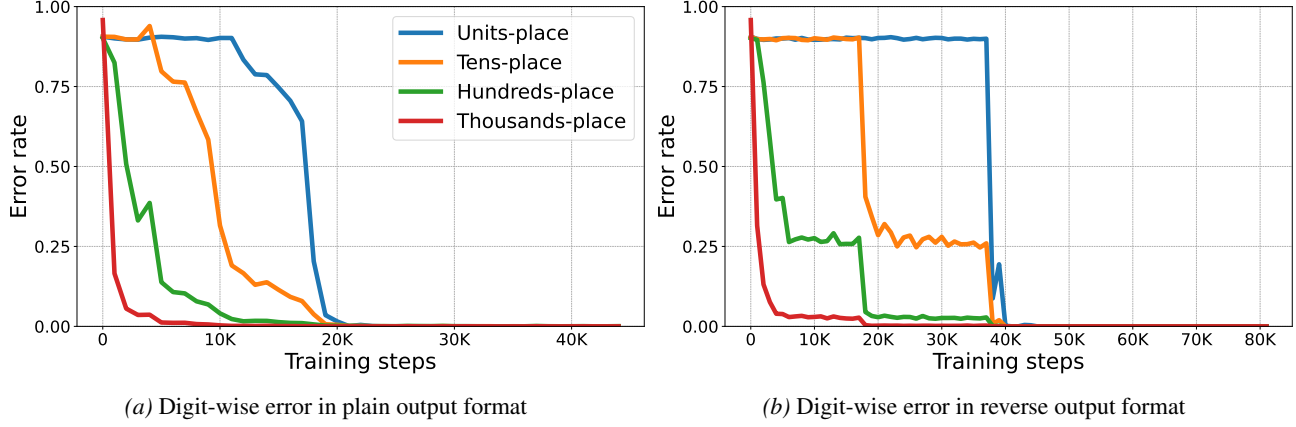


**Figure 10. Using randomly chunked input sequence, transformers still learn digits in non-human order for addition.** We train transformers with randomly chunked blocks as input sequences and evaluate the digit-wise error rates. Same as single-example input sequence format, models learn digits from the most significant digit to the least significant digit.

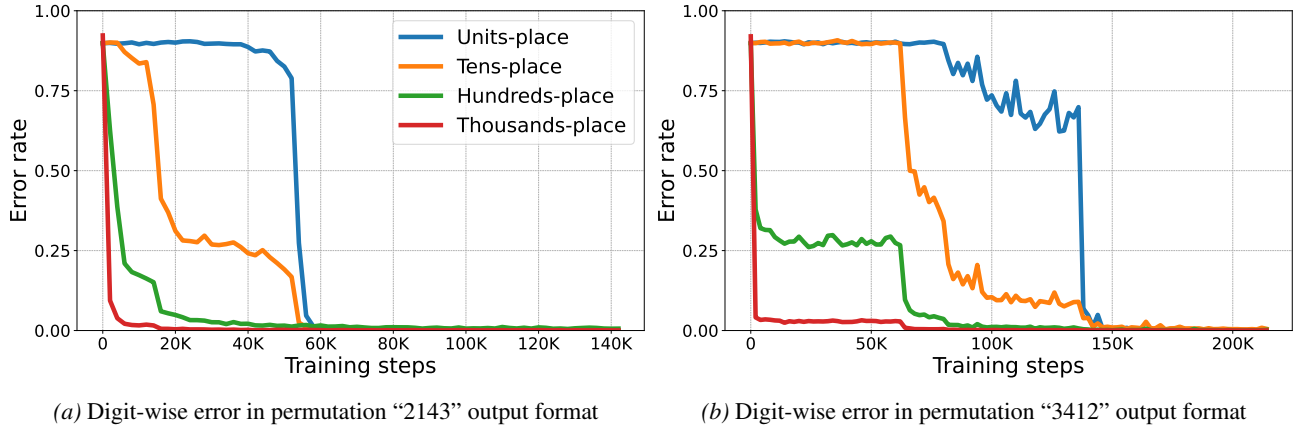


**Figure 11. Regardless of permutations of the output order, transformers learn digits in non-human order for addition.** We train transformers on addition of the format  $a + b + c + d = o$  with the digits of  $o$  written in different permutation orders. In permutation "2143",  $o$  is written as  $o_2o_1o_4o_3$ . In permutation "3412",  $o$  is written as  $o_3o_4o_1o_2$ . Same as plain and reverse output format, models learn digits from the most significant digit ( $o_4$ ) to the least significant digit ( $o_1$ ).

## C. Details and additional results for synthetic experiments

### C.1. Addition task.

#### C.1.1. ALTERNATIVE FORMAT OF INPUT SEQUENCE

As an alternative to the single-example input sequence format adopted in the main paper, we consider the randomly chunked input sequence format—concatenating all training examples and randomly chunking a fixed-size window as an input sequence. As shown in Figure 10, models still learn from the most significant digit to the least significant one.

#### C.1.2. OUTPUT FORMAT PERMUTATION

In the main paper, we train Transformer models on 4 operand addition using both plain and reverse order as the output format. Here we consider two other permutations of output digits order. Concretely, let  $o_1o_2o_3o_4$  be the groundtruth label for a 4 operand addition instance  $a_1a_2a_3a_4 + b_1b_2b_3b_4 + c_1c_2c_3c_4 + d_1d_2d_3d_4$ , with digits ordered from the most significant to the least significant. We consider permutation "2413" and "3412".

For permutation "2413", a training example takes the form:

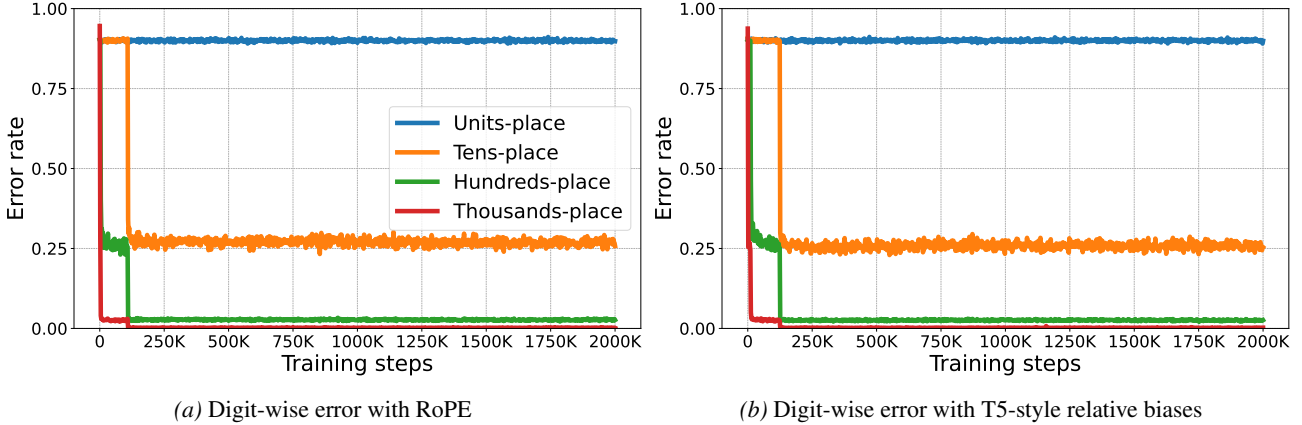


Figure 12. **Additional result for the addition task under two different positional encoding schemes.** We train transformers on 4-operand addition in reverse output format, using RoPE / T5-style relative biases. The units-place error remains high throughout training while tens/hundreds/thousands are learned in reverse order.

$$a_1a_2a_3a_4 + b_1b_2b_3b_4 + c_1c_2c_3c_4 + d_1d_2d_3d_4 = o_2o_1o_4o_3 \quad (1)$$

For permutation “3412”, a training example takes the form:

$$a_1a_2a_3a_4 + b_1b_2b_3b_4 + c_1c_2c_3c_4 + d_1d_2d_3d_4 = o_3o_4o_1o_2 \quad (2)$$

As shown in Figure 11, regardless of the permutation of the output orders, models learn digits from the most significant digit ( $o_4$ ) to the least significant digit ( $o_1$ ).

#### C.1.3. POSITIONAL-ENCODING VARIANTS: ROPE AND T5 RELATIVE

In the main experiments we used absolute positional encodings. To test robustness to positional-encoding choice, we re-ran the 4-operand addition in reverse output format experiment with two alternative encodings: rotary positional embeddings and T5-style relative position biases. Implementation changes were limited to replacing the absolute embedding layer with the alternate encoding described below.

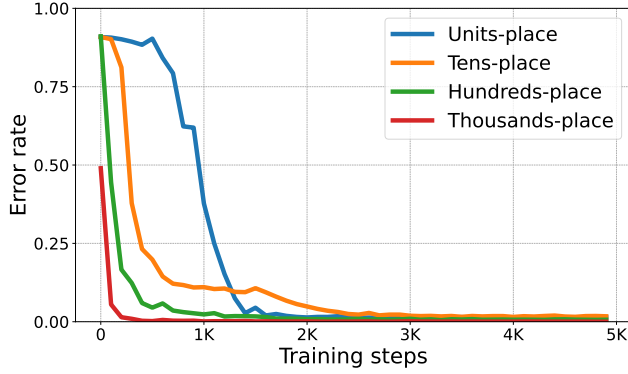
- **RoPE (rotary positional embeddings):** We applied RoPE to the query/key projections following standard practice: a rotary transformation is applied to query and key vectors before computing attention scores.
- **T5-style relative biases:** We implemented learned relative-position bias terms added to the attention logits. The number of relative buckets and max distance were set to 32 and 128 respectively, as are used in the canonical T5 implementation.

Figure 12 shows the digit-wise error rates (units, tens, hundreds, thousands) as training progresses. With both RoPE and T5 relative-position biases the model learns the higher-place digits (tens, hundreds, thousands) in reverse order (i.e., it learns thousands first), but it fails to learn the units-place even after more than 2M training steps.

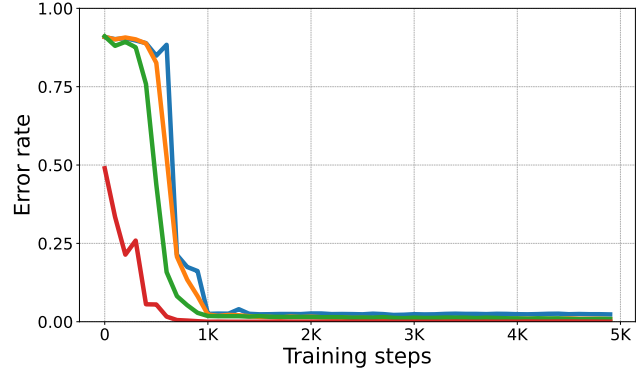
#### C.1.4. GREEDY DECODING

To verify that the choice of generation procedure does not alter the digit-wise learning dynamics we re-ran a suite of experiments using greedy decoding (implemented as top-k decoding with  $k = 1$ ) at evaluation time.

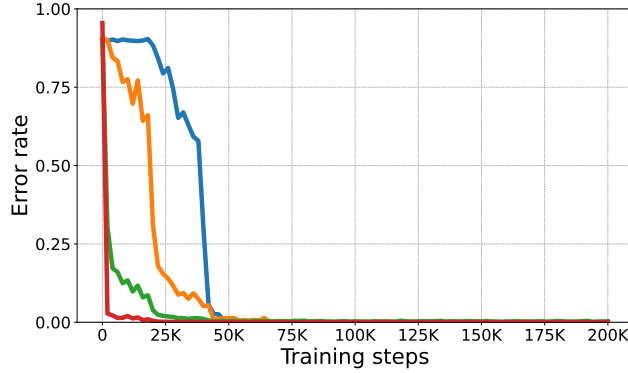
Figure 13 shows that, as in the default sampling setup (temperature 0.8), models evaluated with greedy decoding continue to learn in the non-human order, from the most significant to the least significant digit.



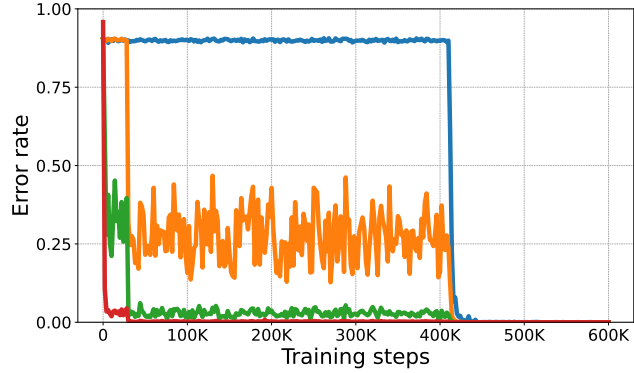
(a) 2-operands addition plain output format with greedy decoding



(b) 2-operands addition reverse output format with greedy decoding



(c) 4-operands addition plain output format with greedy decoding



(d) 4-operands addition reverse output format with greedy decoding

**Figure 13. Results for the addition task under the alternative setup and decoding scheme.** Using greedy decoding, we train transformers on 2-operands and 4-operands addition, in both plain and reverse output format, and evaluate the digit-wise error rate as training progresses. Same as the results obtained under the default setting (with temperature 0.8), models learn digits from the most significant digit to the least significant digit.

### C.1.5. ADDITIONAL ABLATION RESULTS: RANDOMIZING DIGITS

In the main paper we showed the results for randomizing the thousands-place of the output when training addition in the reverse output format. We find similar results when randomizing the hundreds-place of the output. As shown in Figure 14, the model struggles to learn lower digits (tens-place and units-place). When randomizing tens-place in the reverse output format, we find the model is still able to learn the units-place. If randomizing the units-place, the model can learn all the higher digits without difficulty.

We also experimented with ablation when training in the plain format. As shown in Figure 15, when the thousands-place is randomized, the model fails to learn any lower digits. However, when we randomize the hundreds-place, the model still manages to learn the tens-place and units-place, but taking about 5 times longer than without randomization. As a comparison, with the hundreds-place randomized, the model takes around 125K and 200K to learn tens-place and units-place respectively, while without randomization, the model takes only around 25K and 40K steps to learn tens-place and units-place respectively, as shown in the left subplot of Figure 1.

### C.1.6. PREDICTION ERROR DISTRIBUTION AND A NUMERICAL APPROXIMATOR

In the main paper, we aggregated the model’s prediction error counts among the evaluated steps in three chosen windows, which correspond to three stages in learning addition. The reason why we choose to aggregate among a window, instead of just reporting the counts at a single evaluated step, is to smooth out the bumpiness of training dynamics, as we find that for a single training step the mean of the prediction error may swing around 0.

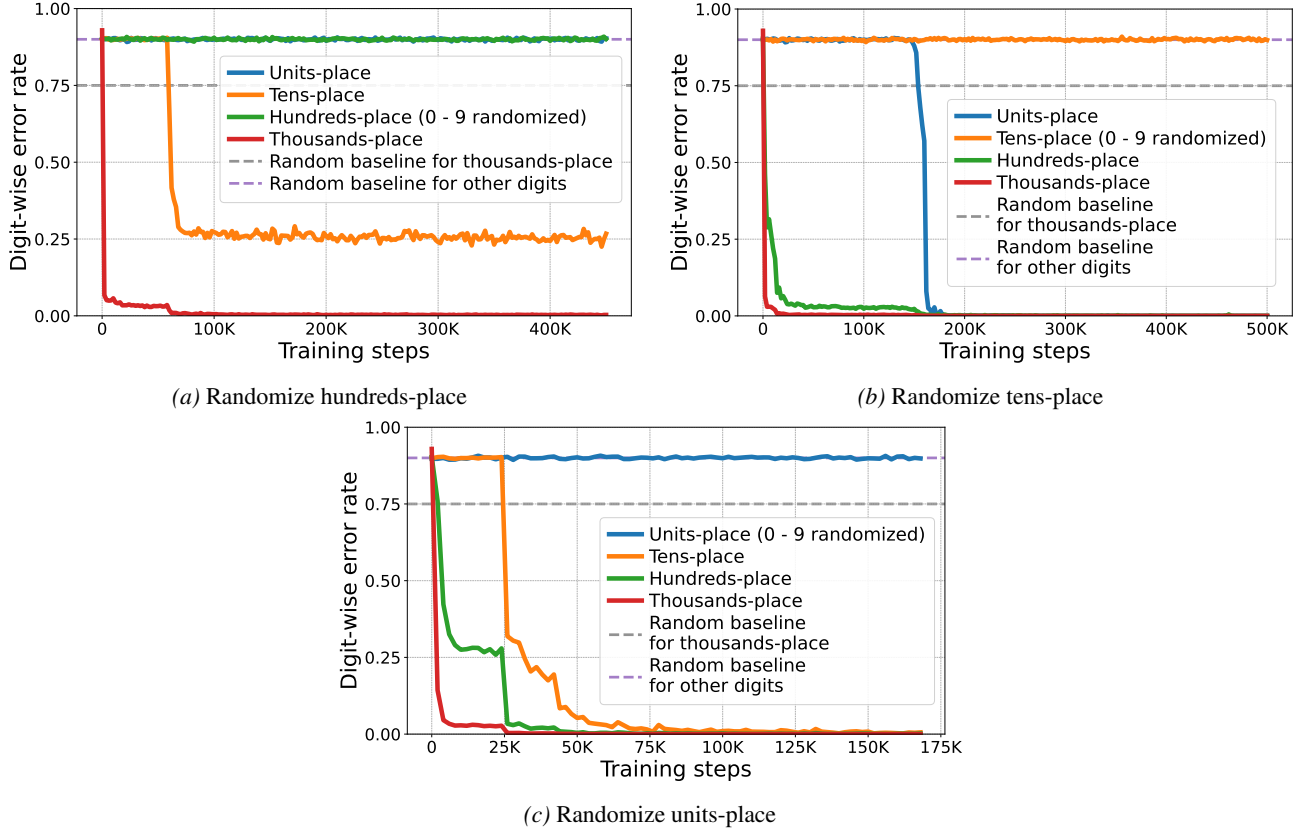


**Figure 14. Ablation experiment results on hundreds-place, tens-place and units-place with the reverse output format.** We train transformers with modified training data for addition with the reverse format, where the hundreds-place digits (a), tens-place digits (b) and units-place digits (c) are replaced by uniform digits in  $\{0, 1, \dots, 9\}$ . Plot (a) shows that the model struggles to learn tens-place digits (error rates above 0.2) and fails to learn the unit-place digits; Plot (b) shows that the model is able to learn the units-place, hundreds- and thousands-place. Plot (c) shows that the model is able to learn all the higher digits without difficulty.

**Error counts.** In Figure 2, we gather the errors on test data from evaluation in three windows, in order to smooth out ‘‘bumpiness’’ of a single checkpoint: (a) left plot: iteration 1K, 1.2K, 1.4K, 1.6K, 1.8K; (b) middle plot: 8K, 10K & 12K. (Note that the x axis range has changed from  $[-800, +800]$  to  $[-100, +100]$ ); (c) right plot: iteration 60K, 62K & 64K.

**Coefficient of determination ( $R^2$ ).** In Figure 2, we reported  $R^2$  scores for each normal fitting. We adopt the following definition of  $R^2$ .

Given observed responses  $\{y_i\}_{i=1}^n$  and corresponding model predictions  $\{\hat{y}_i\}_{i=1}^n$ , we define the residual sum of squares

$$SS_{\text{res}} = \sum_{i=1}^n (y_i - \hat{y}_i)^2$$

and the total sum of squares about the sample mean  $\bar{y} = \frac{1}{n} \sum_{i=1}^n y_i$ ,

$$SS_{\text{tot}} = \sum_{i=1}^n (y_i - \bar{y})^2.$$

The coefficient of determination is

$$R^2 = 1 - \frac{SS_{\text{res}}}{SS_{\text{tot}}}.$$

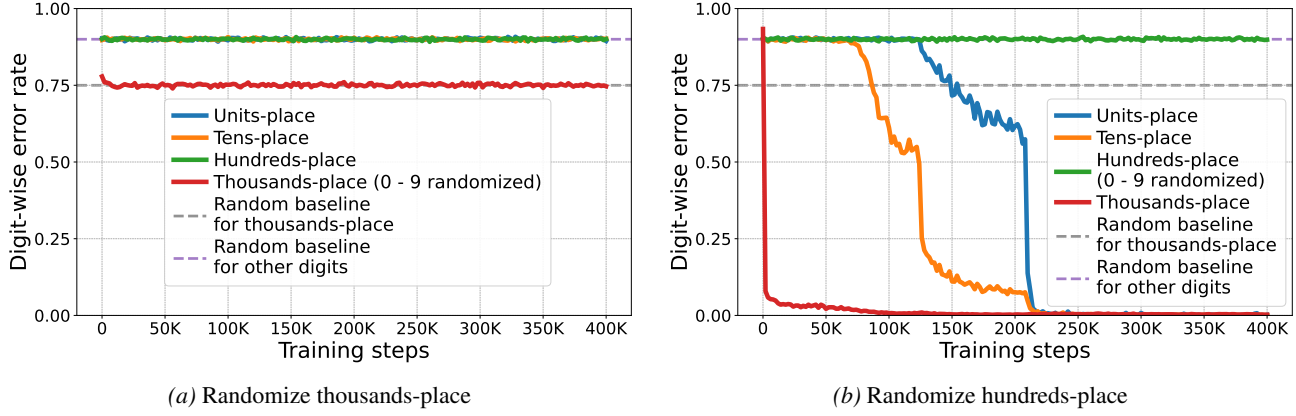


**Figure 15. Ablation experiment results for plain output format addition.** We train transformers with modified training data for addition with the plain format, where the thousands-place digits (left) and hundreds-place digits (right) are replaced by uniform digits in  $\{0, 1, 2, 3\}$  and  $\{0, 1, \dots, 9\}$  respectively. Left plot shows that the model fails to learn any lower digit, whose digit-wise error rates are not better than random baselines. Right plot shows that when randomizing the hundreds-place, the model is still able to learn the tens-place and units-place, but taking about 5 times longer than without randomization.

### C.1.7. ADDITIONAL MUTUAL INFORMATION METRIC RESULTS

In the main paper, we measured the MI  $I(a_1, \hat{p}_0)$  (highest digit) and MI conditioned on the carry to its immediate higher digit  $I(a_i, \hat{p}_i | c_{i-1})$  (other digits), which are compared against the corresponding  $I(a_1, e_0)$  and  $I(a_i, e_i | c_{i-1})$  based on the training data. We showed that the sharp decline of training loss corresponds to the model’s sudden matching with MI metrics at each output digit.

In Figure 16 (right), we also track the MI conditioned on the immediate higher digit  $I(a_i, \hat{p}_i | e_{i-1})$  (for digits other than the highest one), which are compared against the corresponding  $I(a_i, e_i | e_{i-1})$  based on the training data. ( $I(a_2, e_2 | e_1) = 0, I(a_3, e_3 | e_2) = 0$ ) The figure shows that these MI matchings correspond to the sudden drops of the digit-wise error rates as well.

## C.2. Simple Multiplication Task

### C.2.1. ALTERNATIVE FORMAT

In the main paper, we considered training transformers to do 40-digit times 1-digit multiplication in the reverse output format. We also trained models to do the same task but in the plain output format order. As shown in Figure 17, we observed the same learning dynamics as in the reverse output format case—models simultaneously learn the reverse order and normal order.

### C.2.2. OUTPUT FORMAT PERMUTATION

In the main paper, we presented the 40-digit times 1-digit training dynamics results using plain and reverse output format. Following Section C.1.2, we also consider two other permutations of output digits order for our simple multiplication task. One is “block-reversal with rotation”, with the permutation being “11 10 9 8 7 6 5 4 3 2 1 21 20 19 18 17 16 15 14 13 12 31 30 29 28 27 26 25 24 23 22 41 40 39 38 37 36 35 34 33 32”. Another is “odd positions then even positions, reversed evens”, with the permutation being “1 3 5 7 9 11 13 15 17 19 21 23 25 27 29 31 33 35 37 39 41 40 38 36 34 32 30 28 26 24 22 20 18 16 14 12 10 8 6 4 2”. As shown in Figure 18, regardless of the permutation of the output digits, models learn digits in two opposite sequential orders, reverse order and normal order, simultaneously.

### C.2.3. ALTERNATIVE LENGTHS

We also train transformers with 50-digit times 1-digit addition. As in the 40-digit times 1-digit case, transformers learn the reverse order and normal order simultaneously, as shown in Figure 19.

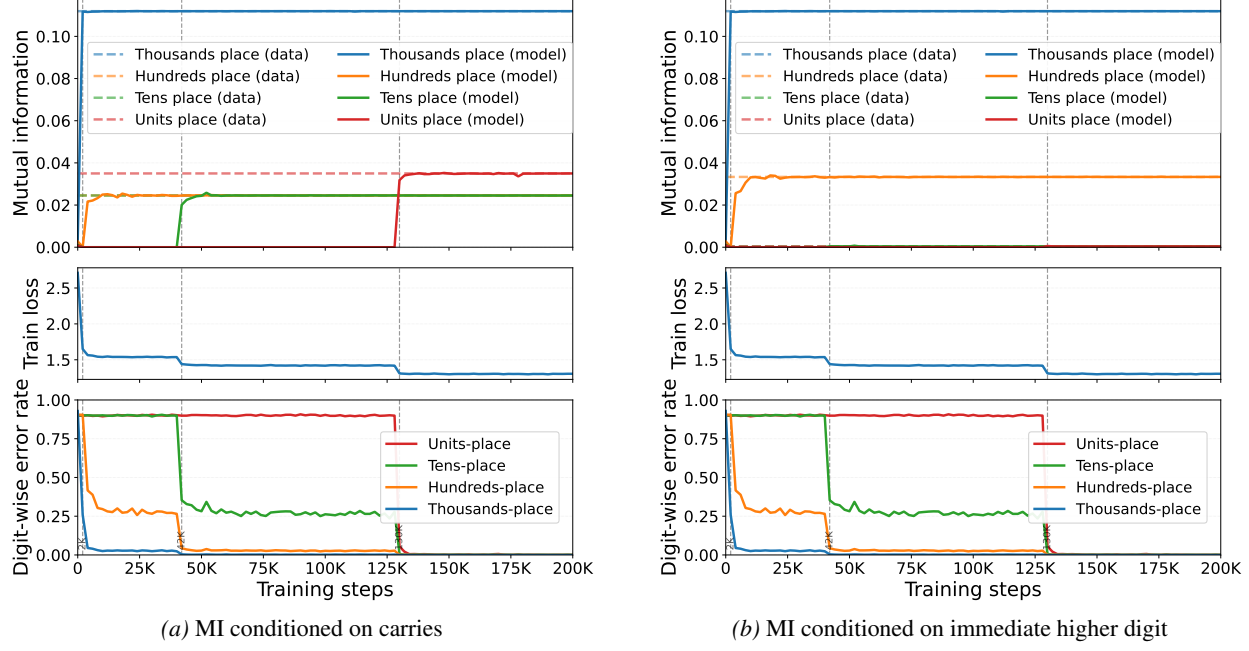


Figure 16. **Left:** In the left top subfigure, we track the MI metrics  $I(a_1, \hat{p}_0)$  (highest digit) and  $I(a_i, \hat{p}_i|c_{i-1})$  (other digits) using the model’s prediction probabilities across training (solid curves), which are compared against the corresponding  $I(a_1, e_0)$  and  $I(a_i, e_i|c_{i-1})$  based on the training data (dashed line). **Right:** In the right top subfigure, we track the MI metrics  $I(a_1, \hat{p}_0)$  (highest digit) and  $I(a_i, \hat{p}_i|e_{i-1})$  (other digits) using the model’s prediction probabilities across training (solid curves), which are compared against the corresponding  $I(a_1, e_0)$  and  $I(a_i, e_i|e_{i-1})$  based on the training data (dashed lines), with  $I(a_2, e_2|e_1) = 0$ ,  $I(a_3, e_3|e_2) = 0$ . The sharp descent of the training loss (middle) and digit-wise error rates (bottom) correspond to the model’s sudden matching with MI metrics at each output digit, indicating skill acquisition.

### C.3. Comparison task.

#### C.3.1. COMPARISON CONTRAST PAIR DATASET

We generate four sets of contrast pairs to isolate the contribution of specific digit positions (see Table 8). The testing pairs  $(a, b)$  in set  $k \in \{1, \dots, 4\}$  differ *strictly* at position  $k$ , while all other digits remain identical. To generate a pair, we first sample a number  $a$  uniformly from  $[1000, 9999]$ . We then construct  $b$  by sampling a digit  $b_k \in \{0, \dots, 9\} \setminus \{a_k\}$  for the  $k$ -th position, setting  $b_i = a_i$  for all  $i \neq k$ . Formally, the condition for set  $k$  is:

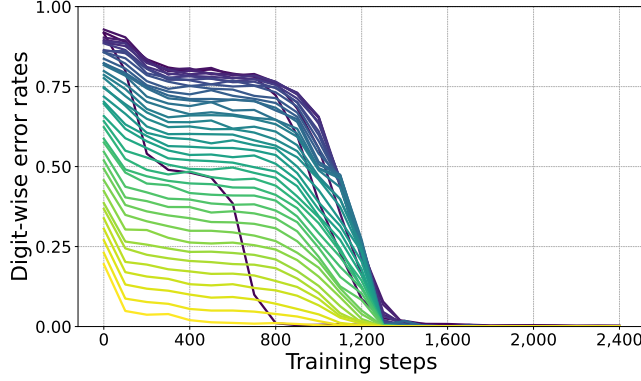
$$a_k \neq b_k \quad \wedge \quad a_i = b_i, \quad \forall i \neq k$$

Table 8. Examples of generated pairs  $(a, b)$  for Comparison Contrast Pair Dataset. For each set  $k$ , the pairs differ *strictly* at the  $k$ -th position (highlighted in bold), while all other digits remain identical.

Set ( $k$ )	Active Position	Constraint	Example a	Example b	Label
1	Thousands	$a_1 \neq b_1; a_{j \neq 1} = b_j$	9 1 5 7	1 1 5 7	>
2	Hundreds	$a_2 \neq b_2; a_{j \neq 2} = b_j$	3 5 5 9	3 <b>9</b> 5 9	<
3	Tens	$a_3 \neq b_3; a_{j \neq 3} = b_j$	7 3 8 9	7 3 <b>3</b> 9	>
4	Units	$a_4 \neq b_4; a_{j \neq 4} = b_j$	5 3 5 0	5 3 5 <b>4</b>	<

#### C.3.2. ADDITIONAL FIGURES

Besides the Contrast Pair Dataset we designed for assessing subskill acquisition, we also use test data of the same distribution as training data (NCID Group 0 to 4). Different NCID groups basically contain numbers of different closeness levels (e.g. models compare 6183 & 6189 in NCID Group 3 while comparing 7291 & 4813 in NCID Group 1). As shown in Figure 20, we find that subskills of comparing numbers of different closeness levels are learned simultaneously.



**Figure 17. With the plain output format, transformers also learn digits in two-way order.** We train transformers on 40-digit times 1-digit multiplication of the format  $a \times b = c$  with the digits of  $c$  written in the plain format (i.e. from the most significant digit to the least significant digit). Same as in the reverse output format case, we find two opposite sequential orders are learned simultaneously. (i) Reverse order: starting from the 41st (highest) digit to the 3rd digit; (ii) Normal order: starting from the 1st (lowest) digit.

#### C.4. Sorting task.

##### C.4.1. UNIFORM SAMPLING

In the sorting task, all training examples take the following format  $a, b, c, d \rightarrow \text{sorted}(a, b, c, d)$ ,

$$\underbrace{9312}_{a}, \underbrace{4661}_{b}, \underbrace{405}_{c}, \underbrace{6252}_{d} \rightarrow \underbrace{405}_{c}, \underbrace{4661}_{b}, \underbrace{6252}_{d}, \underbrace{9312}_{a}.$$

We experimented with different sampling strategies for generating the training dataset. One possible approach is uniform sampling, where  $a, b, c, d$  are uniformly sampled from 0 to 9999. We find under uniform sampling, despite achieving perfect accuracy on the training data distribution, the model performs poorly on sorting

1. **Close numbers:** As described in Section C.4.2, we adopt a suite of specially designed test examples to assess models' subskill learning. Particularly, to measure the 4th digit comparing accuracy we use 4-digit numbers as input, where we controlled the first three digits to be equal. As shown in Figure 21, we find the model's 4th digit accuracy stagnates at around 70%, failing to achieve satisfactory subskill accuracy.
2. **Numbers of distinct lengths:** Considering that under uniform sampling the input numbers range from 0 to 9999, to evaluate the model's length comparing ability, we design the "distinct lengths" test as follows: The 4 input numbers have distinct lengths, being 1-digit, 2-digit, 3-digit, 4-digit respectively. A test example is 15, 4, 5303, 920. However, we find the model fail to acquire this length comparison subskill throughout the training with an accuracy below 10%.

Based on these results, we conclude that uniform sampling is not suitable for models to learn different subskills essential in solving the general sorting task. To expose model more often to training examples of different closeness levels and of varying length we introduced the "doubly balanced" training dataset described in Section A.3.

##### C.4.2. FURTHER DETAILS OF SECTION 4.4

Solving the 4 operand 3-digit & 4-digit sorting task requires the model to master several subskills, combine and apply them in a logical way. These subskills include identifying, then comparing the length of each input number and digit-wise comparison. A more detailed description of these subskills and their logical orders is presented in Table 9. We note that in sorting these subskills have a hierarchical precedence, meaning that the model should apply one subskill only if all previous subskills fail to resolve the ordering.

**Crude length learned first, individual digits learned in parallel** To determine the learning order of these subskills, we use a set of specially targeted tests to assess model's acquisition of each subskill. We summarize each test file and our corresponding evaluation criterion for model's prediction to be counted as correct in Table 10.

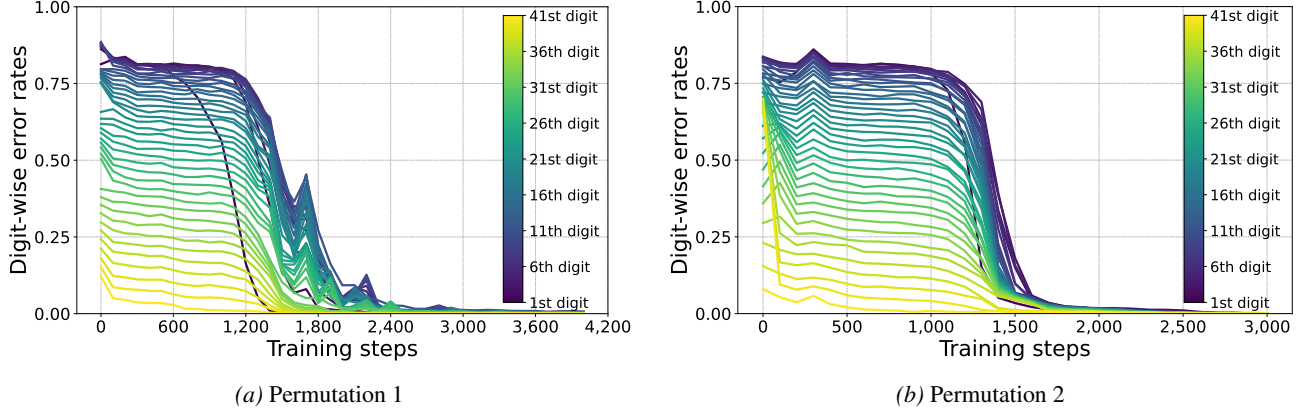


**Figure 18. Regardless of permutations of the output order, transformers learn digits in two-way order for simple multiplication.** We train transformers on simple multiplication of the format  $a \times b = c$  with the digits of  $c$  written in different permutation orders. Following Section C.1.2, we consider two permutation orders rather than plain and reverse format. In the left subfigure, we use the permutation "11 10 9 8 7 6 5 4 3 2 1 21 20 19 18 17 16 15 14 13 12 31 30 29 28 27 26 25 24 23 22 41 40 39 38 37 36 35 34 33 32" (block-reversal with rotation). In the right subfigure, we use the permutation "1 3 5 7 9 11 13 15 17 19 21 23 25 27 29 31 33 35 37 39 41 40 38 36 34 32 30 28 26 24 22 20 18 16 14 12 10 8 6 4 2" (odd positions then even positions, reversed evens). As in plain and reverse output format, we find two opposite sequential orders are learned simultaneously. (i) Reverse order: starting from the 41st (highest) digit to the 3rd digit; (ii) Normal order: starting from the 1st (lowest) digit.

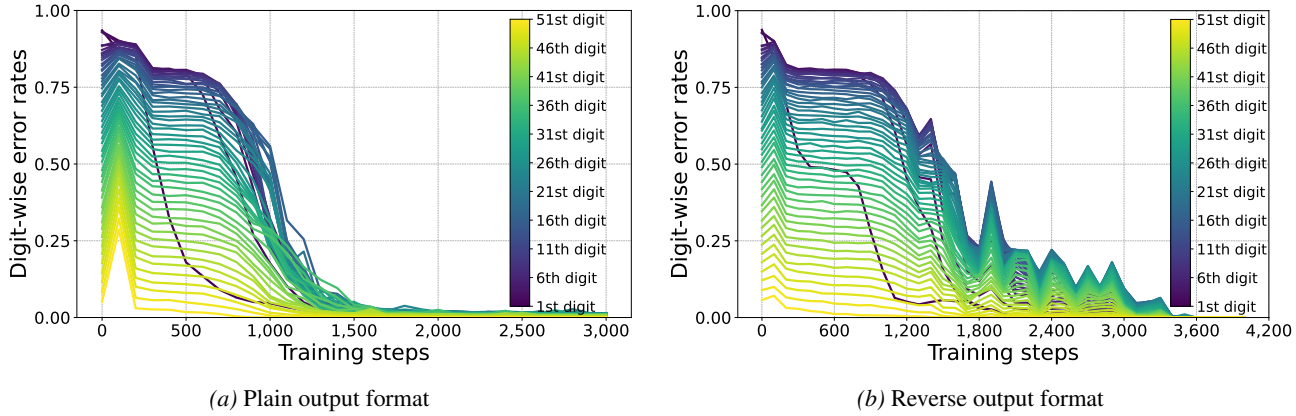


**Figure 19. Simple multiplication: 50-digit times 1-digit results.** Training transformers with 50-digit times 1-digit multiplication, we also find that reverse order and normal order are learned simultaneously.

As shown in Figure 6, the model learns the "crude" length early in training before any digit can be predicted correctly. In other words, at this stage, the model can output the position of the comma, the separating character, correctly. Later, the model learns each individual digit mostly in parallel, with the fourth digit lagging behind.

**Learning different subskills creates competitions.** Solving sorting task requires learning distinct subskills, one sometimes even conflicting with another. We hypothesize that learning one subskill poses challenges to learning other subskills. As a control group to the previously adopted "doubly balanced" training dataset, we design the "closeness-balanced only" training dataset, where all numbers are 4-digit. For each training example, we randomly draw the NCID group from  $k \in \{0, 1, 2\}$ , each with probability 1/3. See Table 11 for details.

Since all input numbers are 4-digit, the model does not need to learn the length comparison subskill. As shown in Figure 22, the model learns 1st digit comparison (subskill 2) significantly earlier when it does not need to learn length comparison (subskill 1). Specifically, when trained with "closeness-balanced only" dataset, it only takes 130 iterations to achieve a 80%+ accuracy. As a comparison, it takes the model 310 iterations to achieve similar performance when trained in the "doubly balanced" dataset.

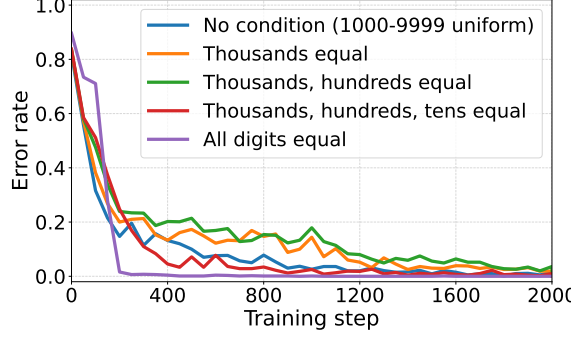


**Figure 20. Transformers learn to compare numbers of different closeness levels concurrently.** When we use test data of the same distribution as training data (NCID Group 0 to 4), we find transformers gain accuracy improvement in all NCID groups simultaneously, which indicates transformers learn to compare numbers of different closeness levels (compare 6183 & 6189 vs compare 7291 & 4813) at the same time.

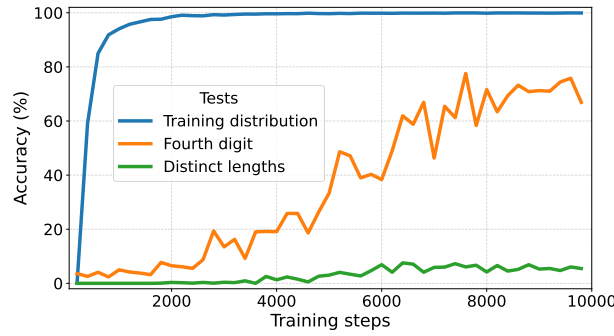


**Figure 21. Under uniform sampling, transformers fail to effectively learn subskills essential in the sorting task.** We train NanoGPTs on 4 operand sorting task. Under uniform sampling, each input number is uniformly sampled from 0 to 9999. Despite achieving a perfect accuracy on the training distribution early in training, the model struggles to compare numbers of distinct lengths and to acquire the 4th digit comparing subskill.

**Models sometimes apply different subskills in undesired ways.** Sorting not only requires models to master different subskills individually, but also to apply them in a logical way. We find during training models are likely to combine different subskills in undesired ways. We design the following three “skewed” test datasets, in all cases one of the input number is 4-digit, the other three numbers are 3-digit:

1. **First digit skewed** The first digit of the 4-digit number is drawn from 1 to 4, while the first digit of the 3-digit numbers is drawn from 5 to 9. The other digits are drawn from 0 to 9. A skewed error in this case is defined as the model outputting the first digit of the 4-digit number as the start of its predicted smallest number. A test example and its corresponding skewed error would be 2774, 524, 996, 875 = 2...
2. **Second digit skewed** The 4 input numbers share the same first digit, which is drawn from 1 to 9. The second digit of the 4-digit number is drawn from 0 to 4, while the second digit of the 3-digit numbers is drawn from 5 to 9. The other digits are drawn from 0 to 9. A skewed error in this case is defined as the model outputting the first two digits of the 4-digit number as the start of its predicted smallest number. A test example and its corresponding skewed error would be 197, 1234, 165, 183 = 12...
3. **Third digit skewed** The 4 input numbers share the same 1st and 2nd digit, which are drawn from 10 to 99. The third digit of the 4-digit number is drawn from 0 to 4, while the third digit of the 3-digit numbers is drawn from 5 to 9. A skewed error in this case is defined as the model outputting the first three digits of the 4-digit number as the start of its predicted smallest number. A test example and its corresponding skewed error would be 787, 789, 7815, 786 = 781...

As shown in Figure 23, the model indeed makes the three kinds of skewed error, with the first kind peaks at even 79% at

Table 9. Subskills required in 3-digit &amp; 4-digit number sorting.

Subskill	Description
Subskill 1	Identify and compare the length of each number
Subskill 2	Compare the 1st digit (apply only if Subskill 1 fail to decide)
Subskill 3	Compare the 2nd digit (apply only if Subskill 1 to 2 fail to decide)
Subskill 4	Compare the 3rd digit (apply only if Subskill 1 to 3 fail to decide)
Subskill 5	Compare the 4th digit (apply only if the number is 4-digit & Subskill 1 to 4 fail to decide)

 Table 10. Test files we use to assess model’s acquisition of different subskills and their corresponding criterion for model’s prediction to be counted as correct.  $l(a, b, c, d)$  denotes the length of the four numbers.

Test file description	Targeted subskill	Criterion
Doubly balanced test	Length Comparison	All Output numbers are of correct lengths
NCID = 0, $l(a, b, c, d) = (4, 4, 4, 4)$	1st digit comparison	Output the 1st digits of the 4 input numbers in correct order
NCID = 1, $l(a, b, c, d) = (4, 4, 4, 4)$	2nd digit comparison	Output the 2nd digits of the 4 input numbers in correct order
NCID = 2, $l(a, b, c, d) = (4, 4, 4, 4)$	3rd digit comparison	Output the 3rd digits of the 4 input numbers in correct order
NCID = 3, $l(a, b, c, d) = (4, 4, 4, 4)$	4th digit comparison	Output the 4th digits of the 4 input numbers in correct order

iteration 150. All three error rates increases at first as the model learns length comparison and digitwise comparison but illogically combining them, then drops as the model figures out how to correctly apply these subskills.

**Additional Mixing Error Analysis** As shown in Table 2, we identified two types of counterintuitive errors models usually make while learning the sorting task. In the main paper, we showed that conflicting digit pairs will exacerbate the mixing error occurrences. Here we investigate the role that same digit pairs play in producing the mixing error effects.

#### SAME-DIGIT TESTS (SD)

These tests vary whether the first and third digit positions are equal across  $b$  and  $c$ , while keeping the (2, 4) conflict present. The goal is to see whether equality at particular positions encourages the model to copy those digits across numbers, producing swaps or repeats.

Test id	Example input	$b_1 = c_1$	$b_3 = c_3$	(2, 4) conflict	Label	Mixing Error	SD
SD1	1000, 6589, 6682, 9999	yes	yes	yes	baseline	6.63%	0.46%
SD2	1000, 6589, 7682, 9999	no	yes	yes	change $b_1$	3.61%	0.32%
SD3	1000, 6589, 6672, 9999	yes	no	yes	change $b_3$	0.0%	0.0%
SD4	1000, 6589, 5672, 9999	no	no	yes	both changed	0.0%	0.0%

**Interpretation:** Compare mixing frequencies across SD1–SD4. Equality at the third digit position ( $b_3 = c_3$ ) appears necessary for mixing to occur. Equality at the first digit ( $b_1 = c_1$ ) amplifies mixing.

**Dynamics of repeating error** When subdividing mixing error into two finer subcategories, swapping and repeating, we find that unlike swapping errors which persist throughout the training process the repeating errors are gradually eliminated. The dynamics of the two types of errors are shown in Figure 24.

## D. Details about GSM8K-based question templates

Most clauses we add can be classified into two types based on how that information is used in the summation. Let  $x_1 + x_2 + \dots + x_i$  be the multi-operand addition we need to perform.

1. **Type 1:** The new term  $x_i$  is a product of two numbers  $a_i$  and  $b_i$  which are directly provided in the new clause. For a concrete example, one original question is "There are 6 boxes of crayons that hold 8 orange crayons. There are 7 boxes of crayons that have 5 blue crayons. There is 1 box of 11 red crayons. How many crayons are there in total?" A  $k = 1$

Table 11. "Closeness-balanced only" training dataset for sorting task. Except that all numbers are 4-digit, all other constraints are the same as in the "doubly balanced" dataset.  $l(a, b, c, d)$  denotes the length of the four numbers.

NCID ( $k$ )	Constraint	Example input
0	$l(a, b, c, d) = (4, 4, 4, 4)$	3621, 7916, 2040, 7304
1	$l(a, b, c, d) = (4, 4, 4, 4); a_1 = b_1 = c_1 = d_1$	7370, 7224, 7141, 7521
2	$l(a, b, c, d) = (4, 4, 4, 4); a_{1:2} = b_{1:2} = c_{1:2} = d_{1:2}$	8168, 8133, 8195, 8174

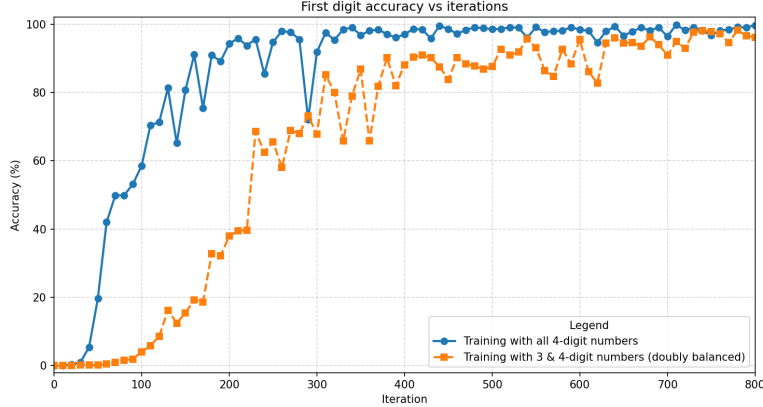


Figure 22. Learning different subskills in sorting creates competition. We train NanoGPTs using either **Blue line**: doubly balanced dataset or **Orange line**: closeness balanced only dataset. Unlike in the doubly balanced dataset where the model needs to learn both comparing length and comparing individual digits, in the closeness balanced only dataset, the model does not need to learn comparing the length, since all numbers are 4-digit. As a result, the model takes much shorter time to achieve 80%+ accuracy in first digit comparison.

extended question would add the clause "There are 4 boxes of crayons that hold 6 green crayons" before asking the total number of crayons.

2. **Type 2:** The new term  $x_i$  must be derived by using information from earlier clauses, thus requiring the model to form a reasoning chain to compute the correct term. For a concrete example, if the original question is "McKenna has 34 stuffed animals. Kenley has twice as many as McKenna. Tenly has 5 more than Kenley. How many stuffed animals do the three girls have in all?" A  $k = 1$  extended question would add the clause "Riley has 10 fewer stuffed animals than Tenly" before asking how many stuffed animals in total these people have.

## D.1. Extended question examples

Here we provide five examples of our extended question with  $k = 6$ .

1. **Example 1:** Original question:

Toulouse has twice as many sheep as Charleston. Charleston has 4 times as many sheep  
 ↳ as Seattle. How many sheep do Toulouse, Charleston, and Seattle have together if  
 ↳ Seattle has 20 sheep?

$k = 6$  extended question:

Toulouse has 2 times as many sheep as Charleston. Charleston has 4 times as many  
 ↳ sheep as Seattle. Seattle has 2 times as many sheep as Alice. Alice has 5  
 ↳ times as many sheep as Bob. Bob has 3 times as many sheep as David. David  
 ↳ has 2 times as many sheep as Zoe. Zoe has 4 times as many sheep as John.  
 ↳ John has 5 times as many sheep as Rachel. How many sheep do Toulouse,  
 ↳ Charleston, Seattle, Alice, Bob, David, Zoe, John and Rachel have together  
 ↳ if Rachel has 20 sheep?

2. **Example 2:** Original question:

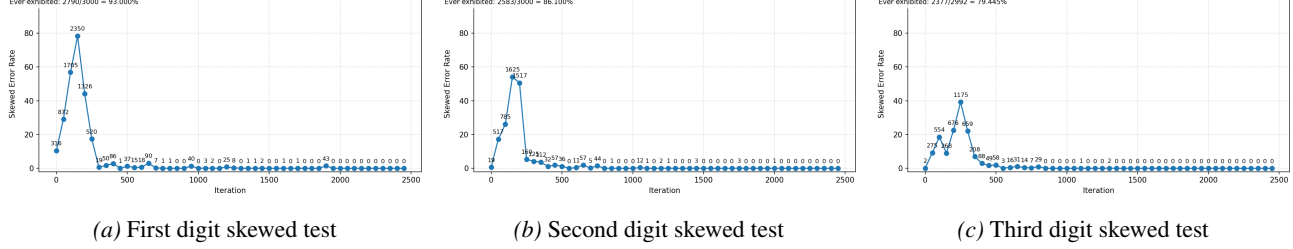


Figure 23. **Transformers apply different subskills in expected ways.** As in Figure 5, we train the model using doubly balanced dataset, which requires the model to master both length comparison and digitwise comparison. We test the model on three datasets, "First digit skewed", "Second digit skewed", and "Third digit skewed". (a) On "First digit skewed" dataset, the model makes errors of the kind 2774, 524, 996, 875 = 2.... At iter 150, the error rate peaks at 78%. (b) On "Second digit skewed" dataset, the model makes errors of the kind 197, 1234, 165, 183 = 12.... At iter 150, the error rate peaks at 54%. (c) On "Third digit skewed" dataset, the model makes errors of the kind 787, 789, 7815, 786 = 781.... At iter 250, the error rate peaks at 39%.

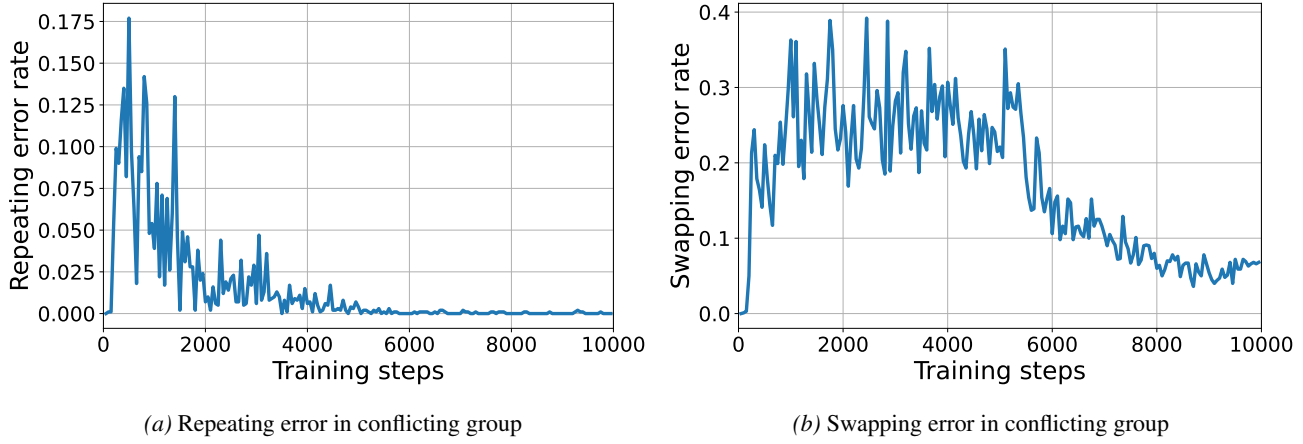


Figure 24. **Repeating errors disappear as training progresses.** In the conflicting test group, models first experience a high rate of repeating error, then gradually eliminates this subcategory of mixing error as we increase the training steps. This contrasts with the swapping error, which persists and converges to around 6% at the end of training.

Henrietta is repainting her house. The walls in the living room take up 600 square feet. She has three bedrooms. The walls in each bedroom take up 400 square feet. If one gallon of paint can cover 600 square feet, how many gallons of paint does Henrietta need to paint her house?

$k = 6$  extended question:

The living room walls take up 600 square feet. The bedroom walls (each) take up 400 square feet and there are 3 of them. The kitchen walls (each) take up 500 square feet and there are 6 of them. The dining room walls (each) take up 240 square feet and there are 5 of them. The bathroom walls (each) take up 150 square feet and there are 8 of them. The garage walls (each) take up 480 square feet and there are 5 of them. The hallway walls (each) take up 900 square feet and there are 8 of them. The sunroom walls (each) take up 300 square feet and there are 6 of them. If one gallon of paint covers 600 square feet, how many gallons of paint does Henrietta need to paint her house?

### 3. Example 3: Original question:

Bill is making omelets for his family's breakfast. It takes him 3 minutes to chop a pepper, 4 minutes to chop an onion, and 1 minute to grate enough cheese for one omelet. It takes him 5 minutes to assemble and cook the omelet. If he needs to chop up four peppers, two onions, and also grates cheese for cooking each of five omelets, how long will he spend preparing for and cooking the five omelets?

$k = 6$  extended question:

Bill is making omelets for his family's breakfast. It takes him 3 minutes to  
 ↳ chop a pepper, 4 minutes to chop an onion, and 1 minute to grate enough  
 ↳ cheese for one omelet. It takes him 5 minutes to assemble and cook one  
 ↳ omelet. He needs to chop up 4 peppers, chop 2 onions, and grate cheese for  
 ↳ cooking each of 5 omelets. He also needs to chop 3 tomatoes, and it takes  
 ↳ him 4 minutes to chop a tomato. It takes him 2 minutes to slice enough  
 ↳ mushrooms for one omelet, and he adds mushrooms to each of the 5 omelets. It  
 ↳ takes him 3 minutes to dice enough ham for one omelet, and he adds ham to  
 ↳ each of the 5 omelets. It takes him 1 minute to rinse a handful of spinach  
 ↳ for one omelet, and he adds spinach to each of the 5 omelets. It takes him 2  
 ↳ minutes to crack and whisk the eggs for one omelet, and he does this  
 ↳ separately for each of the 5 omelets. After he finishes cooking, it takes  
 ↳ him 6 minutes to wash the cutting board and knife. How long will he spend  
 ↳ preparing for and cooking the 5 omelets?

**4. Example 4:** Original question:

In a spelling contest held in her school, Drew got 20 questions correct, winning  
 ↳ her the competition. She got six questions wrong, and her competitor Carla  
 ↳ got 14 questions correct, and twice as many questions wrong as the number of  
 ↳ questions Drew got wrong. If each competitor was asked a different question,  
 ↳ how many questions were asked in the competition?

$k = 6$  extended question:

In a spelling contest held in her school, Drew got 20 questions correct, winning  
 ↳ her the competition. She got six questions wrong, and her competitor Carla  
 ↳ got 14 questions correct and twice as many questions wrong as the number of  
 ↳ questions Drew got wrong. Another competitor, Maya, got 3 fewer questions  
 ↳ correct than Drew and 2 more questions wrong than Drew. Another competitor,  
 ↳ Eli, got 5 more questions correct than Carla and half as many questions  
 ↳ wrong as Carla. Another competitor, Sasha, got twice as many questions  
 ↳ correct as the number of questions Drew got wrong, and she got 4 fewer  
 ↳ questions wrong than Carla. Another competitor, Noah, got the same number of  
 ↳ questions correct as Carla and 3 fewer questions wrong than Drew. Another  
 ↳ competitor, Priya, got 2 fewer questions correct than Eli and 1 more  
 ↳ question wrong than Sasha. Another competitor, Jamal, got 4 fewer questions  
 ↳ correct than Maya and twice as many questions wrong as Noah. If each  
 ↳ competitor was asked a different question, how many questions were asked in  
 ↳ the competition?

**5. Example 5:** Original question:

Buffy has a sailboat with a planing hull that she sails in the Gulf of Mexico.  
 ↳ Under optimal wind conditions, the use of two sails brings the ship to the  
 ↳ speed of 50 knots, whereas under the same conditions, the use of one sail  
 ↳ brings her ship to the speed of 25 knots. A knot is a nautical term for  
 ↳ speed equal to 1 nautical mile per hour, and one nautical mile equals 1.15  
 ↳ land miles. If she travels in her sailboat under optimal wind conditions for  
 ↳ 4 hours with one sail and then for another 4 hours with two sails, what is  
 ↳ the total distance, in land miles, that she will travel?

$k = 6$  extended question:

Buffy has a sailboat with a planing hull that she sails in the Gulf of Mexico. Under optimal wind conditions, the use of two sails brings the ship to the speed of 50 knots, whereas under the same conditions, the use of one sail brings her ship to the speed of 25 knots. A knot is a nautical term for speed equal to 1 nautical mile per hour, and one nautical mile equals 1.15 land miles. If she travels in her sailboat under optimal wind conditions for 4 hours with one sail and then for another 4 hours with two sails, Under the same conditions, the use of three sails brings the ship to the speed of 60 knots, and she sails for 1 hour using three sails. Under the same conditions, the use of four sails brings the ship to the speed of 70 knots, and she sails for 2 hours using four sails. Under the same conditions, sailing with one reefed sail brings her ship to the speed of 15 knots, and she sails for 4 hours with a reefed sail. Under the same conditions, the use of two sails while carrying extra cargo brings her ship to the speed of 40 knots, and she sails for 1 hour using two sails with the extra cargo. Under the same conditions, the use of one sail with a favorable current brings her ship to the speed of 30 knots, and she sails for 2 hours with that setup. Under the same conditions, if she lowers all sails and just drifts, her ship moves at 5 knots, and she drifts for 4 hours. what is the total distance, in land miles, that she will travel?

## D.2. Common Error Types

We examined some failure cases of LLMs in our clause-extended question test. Common types of error include the following.

1. **Direct calculation mistakes in multi-operand addition** Among the error cases, often the model attempts to perform direct addition on multiple operands (in contrast to adding one by one), but made a mistake in its calculation. An example is  $4 + 3 + 2 + 1 + 5 + 3 + 4 + 6 = 32$  inches, where the correct sum should be 28.
2. **Repeating one item** The model sometimes double-counted one term. For example in earlier step it correctly writes the summation it needs to perform as  $64 + 256 + 32 + 32 + 16 + 48 + 64 + 48 + 32$ , but later when adding one by one it writes

```
**Add the numbers step by step:**
- \(\ 64 + 256 = 320 \)
- \(\ 320 + 32 = 352 \)
- \(\ 352 + 32 = 384 \)
- \(\ 384 + 16 = 400 \)
- \(\ 400 + 48 = 448 \)
- \(\ 448 + 64 = 512 \)
- \(\ 512 + 48 = 560 \)
- \(\ 560 + 48 = 608 \) // It double-counted this "48"
- \(\ 608 + 32 = 640 \)
```

3. **Missing one item** Sometimes the LLM does not add all the relevant terms. An example is when earlier it calculated the produce of guavas is 100 kg, but this did not get added in the final summation. When it calculate the total produce of all fruits, it misses this item and writes Total produce =  $400 + 800 + 600 + 700 + 300 + 350 + 200 + 450 = 4000$  kg.
4. **Incorrectly interpreting the units of intermediate results** For example, in earlier step the model calculates one intermediate result to be 42 pills/week. Later when calculating others it uses as 42 pills/day.
5. **Fail to locate effective information** Sometimes the model quotes as irrelevant piece of information as its argument for performing one reasoning. For example, one question says ““Wanda brings half as many treats as Jane”, but the model analyzes that “Jane brings 75% as many pieces of bread as treats. Let  $T_J$  be the number of treats Jane brought. Then:  $T_J = T_W = 30$ ”. To correctly calculate  $T_J$ , it should use the information “Wanda brings half as many treats as Jane” from the question and writes  $T_J = 2 * T_W = 60$  instead.

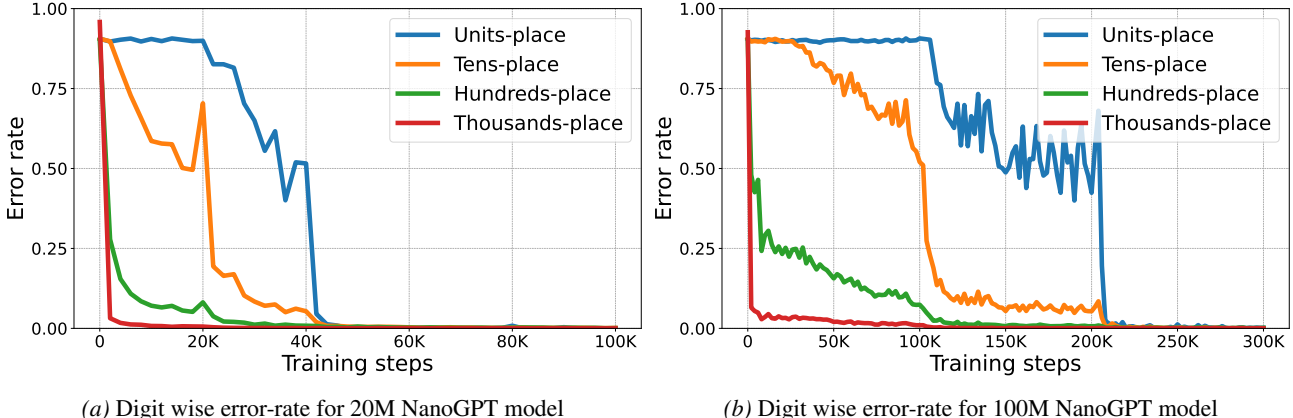


Figure 25. Using larger models to train the addition task from scratch model still learn digits in reverse format. The results are for 20M and 100M NanoGPT models for addition of the format  $a + b + c + d = e$ .

The "direct calculation mistakes" emphasize the challenges for transformer-based models to perform long arithmetic. The other types, such as "repeating/missing one item", bear close resemblance to the mixing errors we observed in the sorting task, indicating the difficulty for transformers to master human-rule compositions.

## E. Details about scaling tests

### E.1. Pure Model scaling

To investigate the effect of model scaling on learning order, we scaled the NanoGPT architecture to 20M and 100M parameters. The architectural details for each model size are presented in Table 4. All three variants were trained using the identical hyperparameters listed in Table 5.

We observed that the number of iterations required to learn the addition task increased as we scaled up the model parameters. However, Figure 25 illustrates that despite this difference in capacity, both the 20M and 100M models exhibited the same reverse digit-wise learning order. These results suggest that parameter scaling does not fundamentally alter the underlying stagewise learning dynamics for arithmetic tasks.

### E.2. Pre-trained Model Fine-tuning

To investigate the effect of pre-training on arithmetic learning dynamics, we fine-tuned the Pythia-1B model on a 4-operand addition task. Prior to fine-tuning, we evaluated the off-the-shelf model on the addition task and the model achieved 0% accuracy, confirming that it possessed no zero-shot capability for this specific task.

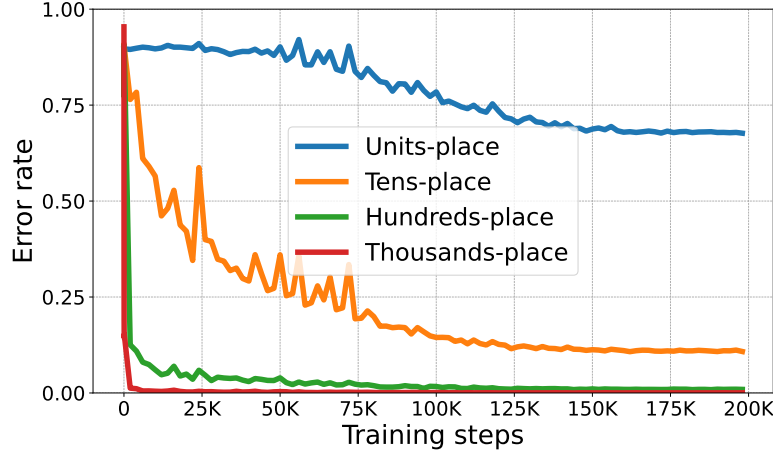
For the fine-tuning process, we utilized a learning rate of  $1 \times 10^{-4}$ . Full details of the training configuration and hyperparameters are provided in Table 5.

We limited the fine-tuning of the pre-trained Pythia-1B model to 200,000 iterations. Although the model did not reach 100% accuracy within this budget, Figure 26 illustrates that the learning dynamics remained consistent with our previous observations. Specifically, the model exhibited the characteristic reverse learning order, prioritizing the acquisition of the most significant digit, signifying that pre-training does not fundamentally alter this learning dynamic.

### E.3. Scratchpad-based Reasoning Training

We employed a scratchpad training strategy to induce intermediate reasoning steps similar to CoT reasoning. We utilized our standard NanoGPT architecture trained with default hyperparameters (refer to Table 4 and Table 5 for full configuration). Here we provide further explanations for the two scratchpad formats.

1. **Direct Decomposition (D scratchpad):** The model decomposes the addends by place value and immediately computes



(a) Digit wise error-rate for Pythia-1B model

Figure 26. Pre-trained model fine-tuned for addition learn digits in non-human order. We fine-tune pythia-1B model on addition of the format  $a + b + c + d = e$  for plain-format. The result shows that pre-training on diverse data doesn't affect how the model internally learns arithmetic tasks.

the final sum.

$$811 + 856 + 239 + 313 = 100(8 + 8 + 2 + 3) + 10(1 + 5 + 3 + 1) + 1(1 + 6 + 9 + 3) = 2219$$

2. **Decomposition plus Aggregation (D+A scratchpad):** The model decomposes the addends and explicitly calculates the sum for each place value group before converging on the final result.

$$\begin{aligned} 811 + 856 + 239 + 313 &= 100(8 + 8 + 2 + 3) + 10(1 + 5 + 3 + 1) + 1(1 + 6 + 9 + 3) \\ &= 100(21) + 10(10) + 1(19) \\ &= 2219 \end{aligned}$$

Both scratchpad formats significantly outperformed standard training, requiring substantially fewer iterations to reach convergence. Specifically, the **Decomposition plus Aggregation (D+A)** scratchpad required only 1,000 iterations and the **Direct Decomposition (D)** format 10,000 iterations, representing a dramatic reduction compared to the approximately 60,000 iterations needed for the standard model. Figure 27 illustrates the distinct learning dynamics for each format:

- **Direct Decomposition (D):** As shown in Figure 27 (a), the model still exhibited the reverse learning order, prioritizing higher-order digits before lower-order ones, mirroring the behavior of the base model.
- **Decomposition plus Aggregation (D+A):** In contrast, Figure 27 (b) reveals that the D+A format altered this dynamic slightly; while it still learned the Most Significant Digit (MSD) first, the remaining three positions were learned nearly simultaneously rather than sequentially.

## F. Proof of Theorem 5.1

*Proof.* **Part 1:** we will show  $I(a_i; e_0) > 0$  for  $i \in \{1, 2, 3\}$ .

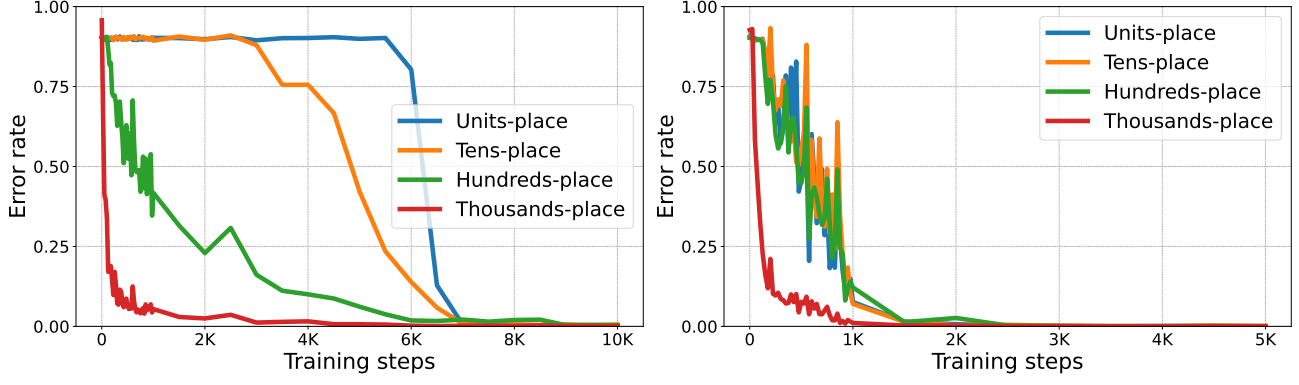
Write the full numbers as  $A, B, C, D \in \{0, \dots, 999\}$ . Let  $S := A + B + C + D$ . By definition  $e_0 \geq 1$  iff  $S \geq 1000$ .

**Case 1:**  $a_1$  (hundreds digit). Write

$$S = 100a_1 + R, \quad R := 10a_2 + a_3 + B + C + D,$$

so  $R$  is independent of  $a_1$ . Then

$$\Pr(e_0 \geq 1 \mid a_1 = 0) = \Pr(R \geq 1000), \quad \Pr(e_0 \geq 1 \mid a_1 = 9) = \Pr(R \geq 100).$$



(a) Digit wise error-rate for Direct Decomposition (D)

(b) Digit wise error-rate for Decompositon plus Aggregation (D+A)

Figure 27. **Scratchpads accelerate convergence but fail to enforce human learning order.** Although scratchpads reduce training steps, neither format successfully restores the Least-to-Most Significant Digit progression inherent to the addition algorithm.

Since  $\{R \geq 1000\} \subseteq \{R \geq 100\}$ , these two probabilities are equal only if  $\Pr(100 \leq R \leq 999) = 0$ . But that event has positive probability: for example the concrete assignment

$$a_2 = 0, a_3 = 0, B = 500, C = 0, D = 0$$

gives  $R = 500$ , so  $\Pr(R = 500) > 0$ . Hence

$$\Pr(R \geq 1000) < \Pr(R \geq 100),$$

so  $\Pr(e_0 \geq 1 \mid a_1 = 0) \neq \Pr(e_0 \geq 1 \mid a_1 = 9)$ . Therefore  $a_1$  and  $e_0$  are not independent and  $I(a_1; e_0) > 0$ .

**Case 2:  $a_2$  (tens digit).** Write

$$S = 10a_2 + R, \quad R := 100a_1 + a_3 + B + C + D,$$

so  $R$  is independent of  $a_2$ . Then

$$\Pr(e_0 \geq 1 \mid a_2 = 0) = \Pr(R \geq 1000), \quad \Pr(e_0 \geq 1 \mid a_2 = 9) = \Pr(R \geq 910).$$

Again  $\{R \geq 1000\} \subseteq \{R \geq 910\}$ ; these probabilities differ if  $\Pr(910 \leq R \leq 999) > 0$ . A concrete realization shows this event has positive probability: take

$$a_1 = 9, a_3 = 0, B = 10, C = 0, D = 0,$$

which yields  $R = 900 + 0 + 10 + 0 + 0 = 910$ . Thus  $\Pr(R = 910) > 0$ , so

$$\Pr(R \geq 1000) < \Pr(R \geq 910),$$

hence  $\Pr(e_0 \geq 1 \mid a_2 = 0) \neq \Pr(e_0 \geq 1 \mid a_2 = 9)$ , and  $I(a_2; e_0) > 0$ .

**Case 3:  $a_3$  (units digit).** Write

$$S = a_3 + R, \quad R := 100a_1 + 10a_2 + B + C + D,$$

so  $R$  is independent of  $a_3$ . Then

$$\Pr(e_0 \geq 1 \mid a_3 = 0) = \Pr(R \geq 1000), \quad \Pr(e_0 \geq 1 \mid a_3 = 9) = \Pr(R \geq 991).$$

These differ if  $\Pr(991 \leq R \leq 999) > 0$ . A concrete example again shows positive probability: take

$$a_1 = 9, a_2 = 0, B = 91, C = 0, D = 0,$$

which yields  $R = 900 + 0 + 91 + 0 + 0 = 991$ . Thus  $\Pr(R = 991) > 0$ , so

$$\Pr(R \geq 1000) < \Pr(R \geq 991),$$

hence  $\Pr(e_0 \geq 1 \mid a_3 = 0) \neq \Pr(e_0 \geq 1 \mid a_3 = 9)$ , and  $I(a_3; e_0) > 0$ .

**Part 2: We will show that  $I(a_i; e_j) = 0$  for  $i, j \in \{1, 2, 3\}$ .**

To avoid a name clash with the digit  $c_i$ , for each place  $i$  let  $C_{\text{in}}^{(i)}$  denote the carry coming into that place from the less-significant places (so  $C_{\text{in}}^{(3)} = 0$ ).

**Group 1:**  $I(a_2; e_1), I(a_3; e_1), I(a_3; e_2)$

We prove the representative case  $I(a_2; e_1) = 0$ . The other two follow by similar arguments. By definition,

$$e_1 = (a_1 + b_1 + c_1 + d_1 + C_{\text{in}}^{(1)}) \pmod{10}$$

where  $C_{\text{in}}^{(1)} = \lfloor \frac{(A \bmod 100) + (B \bmod 100) + (C \bmod 100) + (D \bmod 100)}{100} \rfloor$ .

Let  $S_{100} = (a_1 + b_1 + c_1 + d_1) \pmod{10}$ . Since  $a_1, b_1, c_1, d_1 \sim \text{Uniform}\{0, \dots, 9\}$ , their sum modulo 10 is also uniformly distributed:  $S_{100} \sim \text{Uniform}\{0, \dots, 9\}$ . Observe that the hundreds digits  $\{a_1, b_1, c_1, d_1\}$  are independent of  $a_2$  and the other lower-order digits. Thus:

$$\{a_1, b_1, c_1, d_1\} \perp C_{\text{in}}^{(1)} \quad \text{and} \quad \{a_1, b_1, c_1, d_1\} \perp a_2$$

So  $S_{100}$  is independent of  $C_{\text{in}}^{(1)}$  and  $a_2$ . We evaluate the distribution of  $e_1$  conditioned on  $a_2$ .

$$\begin{aligned} P(e_1 = k \mid a_2 = x) &= \sum_c P(e_1 = k \mid C_{\text{in}}^{(1)} = c, a_2 = x) P(C_{\text{in}}^{(1)} = c \mid a_2 = x) \\ &= \sum_c P(S_{100} \equiv k - c \pmod{10}) P(C_{\text{in}}^{(1)} = c \mid a_2 = x) \\ &= \sum_c \left( \frac{1}{10} \right) P(C_{\text{in}}^{(1)} = c \mid a_2 = x) \\ &= \frac{1}{10} \sum_c P(C_{\text{in}}^{(1)} = c \mid a_2 = x) \\ &= \frac{1}{10} \end{aligned}$$

Since  $P(e_1 = k \mid a_2 = x) = P(e_1 = k) = 1/10$ , the variables  $e_1$  and  $a_2$  are independent. Hence,  $I(a_2, e_1) = 0$ .

**Group 2:**  $I(a_i; e_i) = 0$  for  $i \in \{1, 2, 3\}$

Since all input digits are independent and uniformly distributed, in

$$e_i = (a_i + b_i + c_i + d_i + C_{\text{in}}^{(i)}) \pmod{10},$$

we have specifically:

- $a_i$  is independent of the other hundreds digits  $\{b_i, c_i, d_i\}$ .
- $a_i$  is independent of all tens and ones digits, and therefore  $a_i \perp C_{\text{in}}^{(i)}$ .

Let  $X = (b_i + c_i + d_i + C_{\text{in}}^{(i)}) \pmod{10}$ . Since  $b_i, c_i, d_i$  are independent uniform variables on  $\{0, \dots, 9\}$ , their sum modulo 10 is uniformly distributed. Adding  $C_{\text{in}}^{(i)}$  (which is independent of  $b_i, c_i, d_i$ ) results in a cyclic shift of a uniform distribution, which remains uniform. Thus:

$$X \sim \text{Uniform}\{0, \dots, 9\} \quad \text{and} \quad X \perp a_i$$

We can express  $e_i$  as  $e_i = (a_i + X) \pmod{10}$ . Because  $X$  is a uniform random variable independent of  $a_i$ , the resulting sum  $e_i$  is also uniform and independent of  $a_i$ . Formally, for any  $k, x \in \{0, \dots, 9\}$ :

$$P(e_i = k \mid a_i = x) = P(X \equiv k - x \pmod{10}) = \frac{1}{10} = P(e_i = k)$$

Since the conditional distribution does not depend on  $a_i$ ,  $I(a_i; e_i) = 0$ .

**Group 3:**  $I(a_1; e_2), I(a_1; e_3), I(a_2; e_3)$

For every pair in this group,  $a$  belong to a higher digit place than  $e$ . We prove the representative case  $I(a_1; e_2) = 0$ . As before,

$$e_2 = (a_2 + b_2 + c_2 + d_2 + C_{\text{in}}^{(2)}) \pmod{10},$$

where  $C_{\text{in}}^{(2)}$  is the carry from the units place, determined by  $\{a_3, b_3, c_3, d_3\}$ . Since  $e_2$  is completely determined by digits from the tens place and the ones place, and by definition  $a_1 \perp \{a_2, b_2, c_2, d_2, a_3, b_3, c_3, d_3\}$ ,  $a_1$  and  $e_2$  are independent. Hence,  $I(a_1; e_2) = 0$ .

**Part 3: We will show  $I(a_i; e_i \mid c_{i-1}) > 0$  for  $i = 1, 2, 3$ .**

Fix  $i \in \{1, 2, 3\}$ . Write the local sum at position  $i$  as

$$S = a_i + b_i + c_i + d_i + C_{\text{in}}^{(i)},$$

and set

$$U := b_i + c_i + d_i + C_{\text{in}}^{(i)},$$

so  $S = a_i + U$ . The output digit and carry-out are

$$e_i = S \pmod{10}, \quad c_{i-1} := \left\lfloor \frac{S}{10} \right\rfloor \in \{0, 1, 2, 3\}.$$

First note

$$I(a_i; e_i \mid c_{i-1}) = \mathbb{E}_{c_{i-1}}[I(a_i; e_i \mid c_{i-1} = c)] = \sum_{c \in \{0, 1, 2, 3\}} \Pr(c_{i-1} = c) I(a_i; e_i \mid c_{i-1} = c).$$

Since each term is nonnegative, it suffices to find a single carry value  $c \in \{0, 1, 2, 3\}$  with  $I(a_i; e_i \mid c_{i-1} = c) > 0$ . We take  $c = 0$ .

Condition on  $c_{i-1} = 0$ , i.e.  $S = a_i + U \in \{0, 1, \dots, 9\}$ . Consider two values of  $a_i$ :

(i)  $a_i = 9$  and  $c_{i-1} = 0$ . The inequality  $9 + U \leq 9$  forces  $U \leq 0$ , hence  $U = 0$ . Therefore  $e_i = (9 + 0) \pmod{10} = 9$ , and in particular

$$\Pr(e_i = 0 \mid a_i = 9, c_{i-1} = 0) = 0.$$

(ii)  $a_i = 0$  and  $c_{i-1} = 0$ . By uniform sampling there is positive probability to have  $b_i = c_i = d_i = C_{\text{in}}^{(i)} = 0$ , so  $U = 0$  and thus  $e_i = 0$  occurs with positive probability. Hence

$$\Pr(e_i = 0 \mid a_i = 0, c_{i-1} = 0) > 0.$$

The two conditional probabilities above are different, so the conditional distribution of  $e_i$  given  $(a_i, c_{i-1} = 0)$  depends on  $a_i$ . Thus  $I(a_i; e_i \mid c_{i-1} = 0) > 0$ . Since  $\Pr(c_{i-1} = 0) > 0$ , we conclude

$$I(a_i; e_i \mid c_{i-1}) = \sum_{c \in \{0, 1, 2, 3\}} \Pr(c_{i-1} = c) I(a_i; e_i \mid c_{i-1} = c) \geq \Pr(c_{i-1} = 0) I(a_i; e_i \mid c_{i-1} = 0) > 0.$$

This argument applies for each  $i = 1, 2, 3$ , completing the proof of the theorem.  $\square$